Quantum control for the Zeno effect with noise

Haorui Chen [1] and Shengshi Pang [1,2,*]

[1]*School of Physics, Sun Yat-sen University, Guangzhou, Guangdong 510275, China*
[2]*Hefei National Laboratory, University of Science and Technology of China, Hefei 230088, China*

The quantum Zeno effect is a distinctive phenomenon in quantum mechanics, describing the nontrivial effect of frequent projective measurements on hindering the evolution of a quantum system. However, when subjected to environmental noise, the quantum system may dissipate, and the quantum Zeno effect no longer works. This research starts from the physical mechanism for the decay of the quantum Zeno effect in the presence of noise and investigates the effect of coherent quantum controls on mitigating the decrease of the survival probability that the system stays in the initial state induced by the noise. We derive the decay rate of the survival probability with and without coherent quantum controls in general, and show that when the frequency of the projective measurements is large but finite, proper coherent controls by sufficiently strong Hamiltonians can be designed to decrease the decay rate of the survival probability. A two-level quantum system suffering from typical unitary and nonunitary noise is then considered to demonstrate the effect of the proposed coherent quantum control scheme in protecting the quantum Zeno effect against the noise. The decay rate of the survival probability is obtained in the presence of noise, and the control Hamiltonian is further optimized analytically to minimize the decay rate by a variational approach. The evolution paths of the quantum system with the optimal coherent controls are illustrated numerically for different scenarios to explicitly show how the coherent control scheme works in lowering the decay of survival probability.

I. INTRODUCTION

The quantum Zeno effect is the quantum version of the classical Zeno effect, initially proposed by the ancient Greek philosopher Zeno, who is known for the famous paradoxes such as the "flying arrow" and "Achilles and the tortoise" [1]. Interestingly, while the Zeno effect is a paradox in the classical world hypothesizing that frequent observation can freeze the evolution of a system, which is certainly not possible in real life, the capability of quantum measurements to project quantum systems onto specific states [2] opens up the possibility for realizing the Zeno effect in the quantum realm. As early as 1967, Beskow and Nilsson observed that frequent measurements of the positions of unstable particles in a cloud chamber effectively prevented the decay of the particles [3]. This discovery sparked widespread interest among physicists and mathematicians in the feasibility of the Zeno effect in quantum mechanics, leading to subsequent confirmations of the quantum Zeno effect with different experimental setups and physical systems [4–11] and extensive intriguing theoretical explorations [12–15].

The standard mechanism for realizing the quantum Zeno effect is to freeze the evolution of a quantum system through frequent projective measurements [16–18], similar to the phenomenon in the classical Zeno effect known by the old saying "A watched pot never boils." With further research, Kofman found that the anti-Zeno effect, accelerating the evolution of a quantum system proposed by Kaulakys and Gontis in 1997 in the context of quantum chaos [19], would be a more common phenomenon in the quantum regime [20], in contrast to the quantum Zeno effect. This has made the relation and crossover between quantum Zeno and anti-Zeno effects a hot topic in quantum mechanics [17,18,21]. Moreover, the quantum Zeno effect has been generalized to the quantum Zeno dynamics through performing frequent projective measurements on a proper subspace of a quantum system known as the Zeno subspace, where nontrivial unitary evolution is allowed inside the Zeno subspace while the evolution outside the Zeno subspace is suppressed [18,22–24].

Currently, various approaches to the quantum Zeno effect have been proposed. Based on the characteristic timescales of quantum operations that realize the quantum Zeno effects compared to the timescales of quantum system free evolutions, the quantum Zeno effects can be broadly categorized into pulsed quantum Zeno effects and continuous quantum Zeno effects [7,18,25]. The pulsed quantum Zeno effects are realized through frequent projective measurements as mentioned above or strong unitary operations (often known as unitary kicks), which can be unified with bang-bang control and dynamical decoupling in suppressing the decoherence of open quantum systems [26–28], both equivalent in the Zeno limit [29]. The continuous quantum Zeno effect describes the quantum Zeno effect induced by continuous strong coupling between the main and ancillary systems [22,30], by large dissipations that leads the quantum system to decay into a stable subspace [31,32], by continuous partial measurements [33,34], or by nonselective continuous measurements

---

*pangshsh@mail.sysu.edu.cn

[35–40]. In recent years, intensive research has been dedicated to the connections and unified theoretical frameworks between different manifestations of the quantum Zeno effects [18,22,25,29,41–43]. At the same time, attempts to explore the competition between different methods simultaneously applied in the quantum Zeno effects, e.g., involving both nonselective continuous measurements and large dissipation, has started to emerge [37].

In analogy to many other quantum effects, an essential ingredient to realize the quantum Zeno effect is the coherence of the quantum system, which ensures the probability that the system stays in the initial state decays quadratically with time in a short time interval. However, practical quantum systems are inevitably disturbed by the noise from the environments, and quantum coherence is vulnerable to the detrimental effects such as decoherence, relaxations, and dissipations [44,45] which can spoil the quantum Zeno effects and quantum Zeno dynamics [37,39,46,47]. To protect quantum systems against the noise, quantum techniques such as decoherence-free subspaces [48–50], coherent control schemes [51,52], and quantum error correction codes [53,54] have been developed, and in fact, the quantum Zeno effect is essential to some quantum error correction techniques [29,55–58] underscoring its significance in the realm of quantum information science. The quantum Zeno effect, including the quantum Zeno dynamics, has found versatile applications due to its simplicity and diversity in realization, ranging from realization of decoherence-free subspaces for quantum gates [59] to utilization of classical noise and engineering of non-Markovianity in quantum simulation [60,61], diagnosis of noise correlations between photon polarizations [62], realization of universal quantum control between noninteracting qubits [63], and optimization of quantum algorithms [64], etc.

The reservoir correlation time is critical to the effect of noise on the quantum Zeno effect. For example, Gurvitz [39] found that quantum system can still be frozen if the reservoir correlation time is finite, i.e., the noise is non-Markovian, while the Zeno effect vanishes in the short correlation limit, i.e., the noise is Markovian. In recent years, there has been an increasing interest in research devoted to the quantum Zeno effect in the presence of large Markovian dissipations [37,65,66]. For instance, Popkov *et al.* derived that the effect of strong local dissipation in the Zeno limit is equivalent to Markovian quantum dynamics featuring a renormalized effective Hamiltonian and weak dissipation.

As Markovian noise can spoil the quantum Zeno effect and the survival probability of the initial state decays exponentially with time in the presence of noise, it is an intriguing question whether it is possible and how to decrease the noise-induced decay of the quantum Zeno effect by modulating the dynamics of the quantum system.

In this work, we study these questions in detail by involving Markovian noise in the dynamics of a quantum system. The influence of the noise on the quantum Zeno effects and the decay of quantum systems with noise in the Zeno limit are investigated in general, revealing the potential for decreasing the decay rate of survival probability that the system stays in the initial state by quantum controls. We consider controls on the Hamiltonian of the system to protect the Zeno effect against the noise in this paper, and show that the Hamiltonian

control needs to be strong with a strength proportional to the measurement frequency, which is large but finite in order to decrease the influence of noise on the quantum Zeno effect. We obtain the decay rate of the survival probability in the presence of noise with strong control Hamiltonians in general, and show the conditions on the control Hamiltonian as well as on the frequency of the projective measurements to mitigate the disruption on the quantum Zeno effect caused by the noise. This Hamiltonian control scheme is then applied to a two-level system with typical unitary and nonunitary noise to illustrate the general results. We consider the dephasing and the amplitude damping noise as examples, and obtain the minimum decay rate of the survival probability by optimizing the Hamiltonian controls. The results show that the survival probabilities of the initial state can indeed be increased by the optimized Hamiltonian controls on the quantum system. The evolution paths of the two-level system engineered by the Hamiltonian controls are visualized on the Bloch sphere by numerical simulations to illustrate how the control scheme protects the survival probability against the two types of noise.

The paper is organized as follows. In Sec. II we provide preliminaries for the theory of open quantum systems and the quantum Zeno and anti-Zeno effects. In Sec. III we study the decay of quantum Zeno effect in the presence of Markovian noise, and derive the effective decay rate of the survival probability in the presence of Hamiltonian control, which further shows the conditions on the control Hamiltonian to reduce the decay of the survival probability caused by Markovian noise. Section IV considers a strong Hamiltonian control scheme for a two-level system in the presence of two different types of noise, and obtain the effective decay rate and the optimal Hamiltonian controls for the two types of noise respectively. The optimal control Hamiltonians are further derived analytically, and the physical mechanism for the optimal coherent control schemes to suppress the noise influence on the survival probability is illustrated numerically and analyzed in detail. The paper concludes in Sec. V.

II. PRELIMINARIES

In this section, we briefly introduce the preliminary knowledge of the open quantum system theory and the quantum Zeno effect relevant to the current research.

A. Dynamics of open quantum systems

In a closed quantum system, the evolution of a quantum state is generally described by a unitary transformation,

$$\mathcal{E}[\rho] = U\rho U^{\dagger}, \tag{1}$$

where U is the unitary evolution operator,

$$U = \exp(-iHt), \tag{2}$$

determined by the Hamiltonian H of the system and the evolution time t, However, for an open quantum system exposed to the environment, the dynamics of the system can no longer be described by unitary evolutions because of the inevitable coupling between the system and the environment.

For an open quantum system, by treating the system and environment as a closed joint system, the total Hamiltonian of

the system and the environment can be written as

$$H_{\text{tot}} = H_S + H_E + H_{SE}, \tag{3}$$

where H_S and H_E are the local Hamiltonians which rule the dynamics of system and environment, respectively, and H_{SE} stands for the interaction Hamiltonian between the system and the environment.

Suppose that the system and the environment are initially uncorrelated. The initial joint state of the system and the environment can be written as $\rho_{SE} = \rho_S \otimes \rho_E$, where ρ_S and ρ_E are the density operators of the system and the environment, respectively, and the unitary evolution of the joint state can be written as

$$\mathcal{E}_{(t,0)}[\rho_{SE}] = U(t)(\rho_S \otimes \rho_E)U^\dagger(t). \tag{4}$$

When one is interested in the system only, the joint evolution of the system and environment can be reduced to the system alone by tracing over the degrees of the freedom of the environment,

$$\mathcal{E}_{(t,0)}[\rho_S] = \text{Tr}_E[U(t)(\rho_S \otimes \rho_E)U^\dagger(t)]. \tag{5}$$

The quantum evolution $\mathcal{E}_{(t,0)}$ obtained in Eq. (5) gives the general dynamical process of an open quantum system coupled to the environment.

An important property of a quantum process is the Markovianity based on the completely positive and trace-preserving (CPTP) divisibility of the process. If a quantum process satisfies the CPTP divisibility condition,

$$\mathcal{E}_{(t_n,t_0)} = \mathcal{E}_{(t_n,t_{n-1})}\mathcal{E}_{(t_{n-1},t_{n-2})} \cdots \mathcal{E}_{(t_1,t_0)}, \tag{6}$$

where $t_n \geqslant t_{n-1} \geqslant \cdots \geqslant t_0$ are arbitrary time points and each $\mathcal{E}(t_{k+1}, t_k)$ is a CPTP quantum map, the quantum process $\mathcal{E}(t_n, t_0)$ is called Markovian, otherwise non-Markovian. The Markovianity of quantum dynamics is closely related to the reservoir correlation time, which determines the memory effects of the environment, and dependent on various ingredients such as the dimension of the environment and the strength of interaction between the system and environment [67–69].

According to the open quantum system theory that the Markovian dynamics of an open quantum system can always be described by a Gorini-Kossakowski-Lindblad-Sudarshan master equation [70,71],

$$\frac{d\rho(t)}{dt} = \mathcal{L}_t[\rho(t)] = -i\hbar[H, \rho(t)] + \sum_k \mu_k(t)\mathcal{D}[V_k]\rho(t), \tag{7}$$

where H is the Hamiltonian of the system and $\mathcal{D}[V_k]$ denotes the Lindblad infinitesimal generator for dissipative process induced by the kth noise channel generally in the form

$$\mathcal{D}[V_k] = V_k(\cdot)V_k^\dagger - \tfrac{1}{2}\{V_k^\dagger V_k, \cdot\}, \tag{8}$$

with the Born-Markov approximation [69], where $[\cdot, \cdot]$ and $\{\cdot, \cdot\}$ denote the commutator and the anticommutator, respectively. It can be proven that a quantum process is Markovian if and only if it can be described by a master equation (7) with all coefficients $\mu_k(t)$'s non-negative for any time t [72]. When Markovian noise is considered in the following sections, we use the master equation (7) to involve the noise in the evolution of the quantum system.

B. Zeno and anti-Zeno effect

In this subsection we will briefly introduce the fundamental knowledge about the quantum Zeno and anti-Zeno effects.

Suppose a closed quantum system ruled by a Hamiltonian H is initially prepared in a pure state $|\psi\rangle$. One can perform a projective measurement after an evolution time t of the system to verify whether the system is still in its initial state, and the survival probability is given by

$$p(t) = |\langle\psi|e^{-iHt}|\psi\rangle|^2. \tag{9}$$

If the projective measurement is carried out repetitively at time interval τ during an evolution time t, the final survival probability of the system in the initial state at time t reads

$$P(t) = p(\tau)^{t/\tau}, \tag{10}$$

which can be rewritten as an exponential decay with time t,

$$P(t) = \exp[-\gamma_{\text{eff}}(\tau)t], \tag{11}$$

and $\gamma_{\text{eff}}(\tau)$ is the effective decay rate given by

$$\gamma_{\text{eff}}(\tau) = -\frac{\ln p(\tau)}{\tau}. \tag{12}$$

If the interval τ between two consecutive measurements is short, the probability $p(\tau)$ can be approximated to the second order of τ,

$$p(\tau) \approx 1 - \tau^2\langle\Delta^2 H\rangle, \tag{13}$$

where $\langle\Delta^2 H\rangle = \langle\psi|H^2|\psi\rangle - \langle\psi|H|\psi\rangle^2$ is the variance of the Hamiltonian H with respect to the initial state $|\psi\rangle$. If the time interval τ is so short that $\tau\sqrt{\langle\Delta^2 H\rangle} \ll 1$, the effective decay rate (12) becomes

$$\gamma_{\text{eff}}(\tau) \approx \tau\langle\Delta^2 H\rangle. \tag{14}$$

It is interesting to observe from Eq. (13) that when the frequency of measurements $\nu = \tau^{-1}$ is sufficiently large, i.e., $\tau \to 0$,

$$\gamma_{\text{eff}}(\tau) \to 0. \tag{15}$$

This is the limit of "continuous observation," named by Misra and Sudarshan [16], and the survival probability in this case turns out to be

$$P(t) \to 1, \tag{16}$$

implying that the state of the quantum system almost does not change with time and the quantum evolution freezes. This is the quantum Zeno effect.

Instead, if the frequency of measurements is large but still finite, the effective decay rate will be small but finite, which means that the final survival probability of the initial state will slowly decrease with the evolution time t. If the exponential decay of the survival probability is faster than the natural decay of the quantum system induced by noise, e.g., the amplitude damping, without repetitive measurements, it is called quantum anti-Zeno effect.

In the past few years, it has been extensively investigated how the effective decay rate $\gamma_{\text{eff}}(\tau)$ is influenced by the measurement interval τ in various systems and whether it is possible to restore the natural decay rate γ_{free} given by the Fermi golden rule. The ratio of $\gamma_{\text{eff}}(\tau)$ to γ_{free} is a critical

factor to distinguish between the quantum Zeno effect and the quantum anti-Zeno effect [73,74]: the quantum Zeno effect occurs if $\gamma_{\text{eff}}(\tau)/\gamma_{\text{free}} < 1$, and the quantum anti-Zeno effect occurs if $\gamma_{\text{eff}}(\tau)/\gamma_{\text{free}} > 1$.

III. COHERENT QUANTUM CONTROL SCHEME

In this section we consider a general quantum system with a free Hamiltonian H_0, suffering from Markovian noise and being repetitively observed by a projective measurement. Starting with the most general Markovian noise and its impact on the quantum Zeno effect, our aim is to pursue a quantum control scheme to suppress the influence of noise.

Generally, if the dimension of the system is large enough to prepare a quantum error correction code for the given noise and the initial state of the system happens to live in the code subspace, one can use the syndrome detection and unitary recover operations of the quantum error correction code to protect the Zeno effect. For more general scenarios, this is not always the case, and one needs to resort to other methods to suppress the influence of noise on the Zeno effect. Inspired by the dynamical decoupling method, we explore coherent quantum controls such as Hamiltonian controls to protect the Zeno effect against noise in this paper. The dynamical decoupling requires that the control pulses are performed sufficiently frequently so that the interval between two consecutive control pulses is shorter than the correlation time of the noise. The requirement for the Hamiltonian control to protect the Zeno effect is similar here: as the magnitude of the change of a quantum state by Markovian noise is $O(\tau)$ while the change by a Hamiltonian is of order $O(\tau^2)$ for a short time interval τ between two measurements, the Hamiltonian control needs to be as strong as of order $O(\tau^{-1})$ to suppress the influence of the noise when the frequency of the measurements is large but finite, i.e., τ is small but nonzero. So we will mainly consider strong Hamiltonian controls in this section.

This section provides the necessary conditions for a coherent quantum control scheme to be capable of suppressing the effects of Markovian noise on the quantum Zeno effect and obtain general analytical results for the decay rate of the survival probability in the presence of noise with the Hamiltonian control. Moreover, we propose the ensemble average fidelity as a metric to evaluate the overall performance of the Hamiltonian control in protecting the quantum Zeno effect against noise over all possible initial states of the quantum system.

It is known by the theory of open quantum systems that the evolution of a general quantum system with a Hamiltonian and Markovian noise can be described by the master equation

$$\partial_t \rho(t) = \mathcal{L}_{\text{tot}}[\rho(t)] = \mathcal{L}_H[\rho(t)] + \mathcal{L}_\mu[\rho(t)], \quad (17)$$

where $\mathcal{L}_{\text{tot}}$ is the total generator of the system evolution and $\mathcal{L}_H[\cdot]$, $\mathcal{L}_\mu[\cdot]$ are the generators of the Hamiltonian evolution and the dissipation process, respectively,

$$\mathcal{L}_H[\cdot] = -i[H, \cdot],$$

$$\mathcal{L}_\mu[\cdot] = \sum_k \mu_k \mathcal{D}[V_k](\cdot) = \sum_k \mu_k \left[V_k(\cdot)V_k^\dagger - \frac{1}{2}\{V_k^\dagger V_k, \cdot\} \right].$$
$$(18)$$

The dissipation rates μ_k's are assumed to be non-negative to guarantee the Markovianity of the noise [72]. For the sake of simplicity, we assume that both H and V_k in Eq. (17) are time-independent.

The master Eq. (17) can be formally solved by exponentiating the total Liouvillian $\mathcal{L}_{\text{tot}} = \mathcal{L}_H + \mathcal{L}_\mu$,

$$\rho(t) = e^{\mathcal{L}_{\text{tot}}t}[\rho(0)], \quad (19)$$

and the survival probability of the initial state of the quantum system after an evolution of time t under the Hamiltonian and the noise between two consecutive measurements in the quantum Zeno effect is given by

$$p(t) = \langle \psi_0 | \rho(t) | \psi_0 \rangle, \quad (20)$$

where $|\psi_0\rangle$ is the initial state of the quantum system and $\rho(0)$ is the density matrix of the initial state, $\rho(0) = |\psi_0\rangle\langle\psi_0|$.

A. Control-free scheme

Before introducing quantum controls to reduce the impact of noise on the quantum Zeno effect, a general quantum system with a free evolution Hamiltonian is considered in this subsection to see the behavior of the final survival probability of the quantum system to stay in the initial state after repetitive projective measurements in the Zeno limit without the protection by quantum control against the noise.

The survival probability after an evolution of τ under the master Eq. (17) followed by a single measurement can be written as

$$p_{\text{n}}(\tau) = \langle \psi_0 | e^{\mathcal{L}_{\text{tot}}^{(\text{n})}\tau}[\rho_0] | \psi_0 \rangle$$
$$= \langle \psi_0 | e^{(\mathcal{L}_{H_0} + \mathcal{L}_\mu)\tau}[\rho_0] | \psi_0 \rangle, \quad (21)$$

where the subscript "n" denotes the absence of quantum control to distinguish from the case with quantum control below.

When the time interval τ between two consecutive measurements is short, the short-time behavior of $p_{\text{n}}(\tau)$ can be obtained by Taylor expansion to the second order of τ,

$$p_{\text{n}}(\tau) = 1 + \langle \psi_0 | \mathcal{L}_\mu[\rho_0] | \psi_0 \rangle \tau$$
$$+ \frac{1}{2} \langle \psi_0 | (\mathcal{L}_{H_0} + \mathcal{L}_\mu)^2[\rho_0] | \psi_0 \rangle \tau^2 + O(\tau^3). \quad (22)$$

There should have been another term $\langle \psi_0 | \mathcal{L}_{H_0}[\rho_0] | \psi_0 \rangle$ in the first-order coefficient, but it has been dropped as it is always zero considering $\mathcal{L}_{H_0}$ is a commutator and $\rho_0 = |\psi_0\rangle\langle\psi_0|$. When the projective measurement is performed repetitively, the final survival probability of the system in the initial state after an evolution time t can be obtained as

$$P_{\text{n}}(t) = p_{\text{n}}(\tau)^{t/\tau} = \exp\left[-\gamma_{\text{eff}}(\tau)t\right], \quad (23)$$

where the subscript "n" in $P_{\text{n}}(t)$ also denotes the absence of quantum control and $\gamma_{\text{eff}}(\tau)$ is the effective decay rate of the system,

$$\gamma_{\text{eff}}(\tau) = -\frac{\ln p(\tau)}{\tau}. \quad (24)$$

Substituting Eq. (22) into $\gamma_{\text{eff}}(\tau)$, one can obtain the approximation of $\gamma_{\text{eff}}(\tau)$ to the first order of τ as

$$\gamma_{\text{eff}}^{(\text{n})}(\tau) = -\langle \mathcal{L}_\mu \rangle - \frac{1}{2}\langle \Delta^2(\mathcal{L}_{H_0} + \mathcal{L}_\mu) \rangle \tau + O(\tau^2). \quad (25)$$

The superscript "(n)" denotes the absence of quantum control, and $\langle \mathcal{L}_\mu \rangle$, $\langle \Delta^2 (\mathcal{L}_{H_0} + \mathcal{L}_\mu) \rangle$ denotes the mean and the variance of the superoperator $\mathcal{L}$ in the Liouville space, respectively [75], with

$$\langle \Delta^2 \mathcal{L} \rangle \equiv \langle \mathcal{L}^2 \rangle - \langle \mathcal{L} \rangle^2 \tag{26}$$

and

$$\langle \mathcal{L}^k \rangle = \langle \psi_0 | \mathcal{L}^k [\rho_0] | \psi_0 \rangle = \mathrm{Tr}(\rho_0 \mathcal{L}^k [\rho_0]) = \langle \vec{\rho_0} | L^k | \vec{\rho_0} \rangle, \tag{27}$$

where the operator L in the Roman font and the ket $|\vec{\rho_0}\rangle$ denotes the matrix form of the superoperator $\mathcal{L}$ and the vector form of the density operator ρ_0 in the Liouville space, respectively. Note this variance of the superoperator $\mathcal{L}$ does not always remain non-negative as $\mathcal{L}$ is not necessarily Hermitian.

It can be further seen from Eq. (25) that when the frequency of measurements $\nu = \tau^{-1}$ is sufficiently large,

$$\nu \gg \left| \frac{\langle \Delta^2 (\mathcal{L}_{H_0} + \mathcal{L}_\mu) \rangle}{2 \langle \mathcal{L}_\mu \rangle} \right|, \tag{28}$$

the linear term of $\gamma_{\mathrm{eff}}(\tau)$ in Eq. (25) becomes negligible and the effective decay rate becomes independent of τ. Note that the condition (28) does not diverge as $\langle \psi_0 | \mathcal{L}_\mu [\rho_0] | \psi_0 \rangle$ is generally nonzero. Consequently, the final survival probability after an evolution of time t can be approximated as

$$P_\mathrm{n}(t) = e^{-\gamma_{\mathrm{eff}}^{(\mathrm{n})} t}, \tag{29}$$

where

$$\gamma_{\mathrm{eff}}^{(\mathrm{n})} \approx -\langle \psi_0 | \mathcal{L}_\mu [\rho_0] | \psi_0 \rangle$$
$$= \sum_k \mu_k [\langle \psi_0 | V_k^\dagger V_k | \psi_0 \rangle - \langle \psi_0 | V_k^\dagger | \psi_0 \rangle \langle \psi_0 | V_k | \psi_0 \rangle]. \tag{30}$$

Note that $\gamma_{\mathrm{eff}}^{(\mathrm{n})}$ is always non-negative due to the Cauchy-Schwarz inequality and the non-negativity of μ_k's.

An important feature of the effective decay rate $\gamma_{\mathrm{eff}}^{(\mathrm{n})}$ (30) is its independence of the time interval τ between two consecutive projective measurements due to the appearance of the linear term in the expansion of $p_\mathrm{n}(\tau)$, which implies that the decay rate does not vanish when $\tau \to 0$ and the survival probability always decays with time in this case. This is in sharp contrast to the quantum Zeno effect where the effective decay rate (14) is proportional to τ and vanishes when $\tau \to 0$. It results in the failure to freeze the evolution of the quantum system in the presence of Markovian noise, implying the quantum Zeno effect vanishes in this case, which is consistent with the results in the existing literature, e.g., [38,39,46].

B. Coherent control scheme

As Markovian noise makes the survival probability of the system to stay in the initial state to decay exponentially even with frequent projective measurements, it is desirable to protect the Zeno effect against the noise with proper quantum control method. From the results in the preceding subsection, it can be seen that the key to the exponential decay of the survival probability lies in the the linear term of the survival probability in the Taylor expansion introduced by the noise after a single step of evolution and projective measurement. So the aim of the quantum control is to decrease the linear
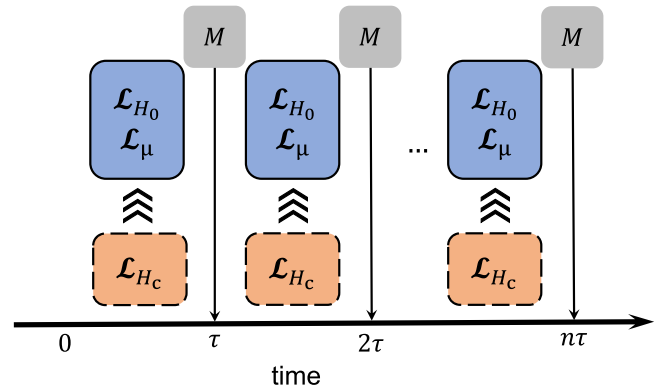

FIG. 1. Scheme of the coherent-control-enhanced quantum Zeno effect in the presence of Markovian noise. In the absence of quantum control, the quantum system undergoes a free unitary evolution and noise simultaneously. At the end of each time interval τ, a projective measurement is performed to observe if the system remains in its initial state. The projective measurement is assumed to be instantaneous, implying no evolution occurs during the measurement process. This process repeats every time interval τ. In the presence of a coherent quantum control, a proper additional control Hamiltonian is applied on the quantum system to engineer the dynamics of the system so that the effective decay rate of the survival probability can be decreased. The projective measurement is denoted by M, and the evolution of free Hamiltonian, the noise and the control Hamiltonian are denoted by $\mathcal{L}_{H_0}$, $\mathcal{L}_\mu$, and $\mathcal{L}_{H_c}$, respectively.

term in the survival probability of a single step of evolution and measurement.

In this subsection, we consider a coherent quantum control scheme to suppress the influence of noise on the quantum Zeno effect and decrease the decay rate of the survival probability of the system in the initial state. The evolution of the quantum system with a coherent control scheme in the presence of noise is illustrated in Fig. 1.

It should be noted that within a short but finite time interval τ, the change of the survival probability by a Hamiltonian is $O(\tau^2)$ (13) but the change of the survival probability by Markovian noise is $O(\tau)$ (22), so if the purpose of a control Hamiltonian is to suppress the effect of noise on the survival probability, the control Hamiltonian needs to be sufficiently strong. As shown in the following, the control Hamiltonian actually needs to be as strong as $O(\tau^{-1})$ to slow the decay of the survival probability, which means the total change of the system induced by the control Hamiltonian over the short time interval τ is approximately $O(1)$, which is similar to those fast pulse controls such as dynamical decoupling and quantum control by reverse optimized pulse sequences [26,47,76].

Suppose a control Hamiltonian gH_c is performed on the quantum system in the presence of noise, where g is the strength parameter. When the measurement interval is τ, the short-time survival probability of the initial state with the Hamiltonian control after a single measurement reads

$$p_\mathrm{c}(\tau) = \langle \psi_0 | e^{\mathcal{L}_{\mathrm{tot}} \tau} [\rho_0] | \psi_0 \rangle$$
$$= \langle \psi_0 | e^{(\mathcal{L}_{H_0} + \mathcal{L}_\mu + g \mathcal{L}_{H_c}) \tau} [\rho_0] | \psi_0 \rangle, \tag{31}$$

where the subscript "c" in $p_\mathrm{c}(\tau)$ denotes the presence of coherent quantum control.

To explore how strong the control Hamiltonian needs to be to suppress the influence of the Markovian noise, we try the ansatz $g = \omega\tau^k$, and the task is to find appropriate choices of k to increase the higher-order terms of the short-time survival probability to the first order of τ. Note that in this case $\mathcal{L}_{\text{tot}}$ will be dependent on τ, so in the following we will denote $\mathcal{L}_{\text{tot}}^{(c)}$ as $\mathcal{L}_{\text{tot}}^{(c)}(\tau)$ to explicitly indicate its dependence on τ with the control Hamiltonian applied. But $\mathcal{L}_{\text{tot}}^{(c)}(\tau)$ is still independent of the instantaneous time points during the evolution as τ is just the time interval between two consecutive projective measurements which can be taken as a parameter, so the evolution under $\mathcal{L}_{\text{tot}}^{(c)}(\tau)$ between two measurements can still be written as $e^{\tau\mathcal{L}_{\text{tot}}^{(c)}(\tau)}$.

It is difficult to directly expand $p_c(\tau)$ with respect to τ by the Taylor expansion of the evolution superoperator $e^{\tau\mathcal{L}_{\text{tot}}^{(c)}(\tau)}$ analogous to Eq. (22),

$$e^{\tau\mathcal{L}_{\text{tot}}^{(c)}(\tau)} = \sum_j \frac{\left(\mathcal{L}_{H_0}\tau + \mathcal{L}_\mu\tau + \omega\tau^{k+1}\mathcal{L}_{H_c}\right)^j}{j!}, \quad (32)$$

since $\mathcal{L}_{H_0}\tau + \mathcal{L}_\mu\tau + \omega\tau^{k+1}\mathcal{L}_{H_c}$ is not proportional to τ here, and all the terms of this expansion include the lowest-order terms of τ. Therefore, we turn to compute the first few derivatives of $e^{\tau\mathcal{L}_{\text{tot}}^{(c)}(\tau)}$ with respect to τ to give the leading terms in the expansion of $p_c(\tau)$. In this case the evolution superoperator $e^{\tau\mathcal{L}_{\text{tot}}^{(c)}(\tau)}$ can be expanded at $\tau = 0$ as

$$e^{\tau\mathcal{L}_{\text{tot}}^{(c)}(\tau)} = e^{\tau\mathcal{L}_{\text{tot}}^{(c)}(\tau)}\big|_{\tau=0} + \tau\partial_\tau\left(e^{\tau\mathcal{L}_{\text{tot}}^{(c)}(\tau)}\right)\big|_{\tau=0}$$
$$+ \frac{\tau^2}{2}\partial_\tau^2\left(e^{\tau\mathcal{L}_{\text{tot}}^{(c)}(\tau)}\right)\big|_{\tau=0} + O(\tau^3). \quad (33)$$

Substituting $g = \omega\tau^k$ into the evolution superoperator $e^{\tau\mathcal{L}_{\text{tot}}^{(c)}(\tau)}$ (33) in the Liouville space, the first-order derivative of $e^{\mathcal{L}\tau}$ [77] can be derived as

$$\partial_\tau e^{\tau\mathcal{L}_{\text{tot}}^{(c)}(\tau)} = \int_0^1 e^{\tau\mathcal{L}_{\text{tot}}^{(c)}(\tau)(1-\eta)}\partial_\tau\left[\tau\mathcal{L}_{\text{tot}}^{(c)}(\tau)\right]e^{\tau\mathcal{L}_{\text{tot}}^{(c)}(\tau)\eta}\,d\eta. \quad (34)$$

At $\tau = 0$ where the evolution superoperator $e^{\tau\mathcal{L}_{\text{tot}}^{(c)}(\tau)}$ is expanded,

$$\tau\mathcal{L}_{\text{tot}}^{(c)}(\tau)\big|_{\tau=0} = \omega\mathcal{L}_{H_c}\tau^{k+1}\big|_{\tau=0},$$
$$\partial_\tau\left[\tau\mathcal{L}_{\text{tot}}^{(c)}(\tau)\right]\big|_{\tau=0} = (k+1)\omega\mathcal{L}_{H_c}\tau^k\big|_{\tau=0} + \mathcal{L}_\mu + \mathcal{L}_{H_0}. \quad (35)$$

It can be observed that if $k > 0$, $\tau\mathcal{L}_{\text{tot}}^{(c)}(\tau)|_{\tau=0} = 0$ and $\partial_\tau[\tau\mathcal{L}_{\text{tot}}^{(c)}(\tau)]|_{\tau=0} = \mathcal{L}_\mu + \mathcal{L}_{H_0}$, so Eq. (34) can be simplified to

$$\partial_\tau\left(e^{\tau\mathcal{L}_{\text{tot}}^{(c)}(\tau)}\right)\big|_{\tau=0} = \partial_\tau\left[\tau\mathcal{L}_{\text{tot}}^{(c)}(\tau)\right]\big|_{\tau=0} = \mathcal{L}_\mu + \mathcal{L}_{H_0}. \quad (36)$$

In this case the first-order terms of $e^{\tau\mathcal{L}_{\text{tot}}^{(c)}(\tau)}$ and of the short-time survival probability $p_c(\tau)$ are independent of the control Hamiltonian H_c, so H_c cannot help decrease the decay rate of the survival probability in the long-term evolution.

If $-1 < k \leqslant 0$, $\tau\mathcal{L}_{\text{tot}}^{(c)}(\tau)|_{\tau=0}$ is still zero, but $\partial_\tau[\tau\mathcal{L}_{\text{tot}}^{(c)}(\tau)]|_{\tau=0}$ includes the control Hamiltonian now. It seems that the Hamiltonian control is possible to decrease the decay rate of the survival probability in this case.

Nevertheless, it can be verified that for any arbitrary initial state $|\psi_0\rangle$,

$$\langle\psi_0|\mathcal{L}_{H_c}[\rho_0]|\psi_0\rangle = 0, \quad (37)$$

so the decay rate can still not be lowered by the Hamiltonian control in this case.

If $k < -1$, it can be immediately inferred from Eq. (35) that both $\tau\mathcal{L}_{\text{tot}}^{(c)}(\tau)$ and $\partial_\tau[\tau\mathcal{L}_{\text{tot}}^{(c)}(\tau)]$ diverge at $\tau = 0$. So the only possible choice of k to make the Hamiltonian control scheme to work is $k = -1$, i.e., the strength parameter of the control Hamiltonian is

$$g = \omega\tau^{-1}. \quad (38)$$

In this case,

$$\tau\mathcal{L}_{\text{tot}}^{(c)}(\tau)\big|_{\tau=0} = \omega\mathcal{L}_{H_c},$$
$$\partial_\tau\left[\tau\mathcal{L}_{\text{tot}}^{(c)}(\tau)\right]\big|_{\tau=0} = \mathcal{L}_\mu + \mathcal{L}_{H_0}, \quad (39)$$

where $\tau\mathcal{L}_{\text{tot}}^{(c)}(\tau)|_{\tau=0}$ includes the control Hamiltonian now, so it is possible to modulate the first-order derivative of $e^{\tau\mathcal{L}_{\text{tot}}^{(c)}(\tau)}$ by the coherent control scheme. Hence, within the framework of coherent control schemes, the strength of the control Hamiltonian needs to be proportional to the frequency of the repetitive projective measurements. This means that the total change of the system made by the control Hamiltonian is of order $O(1)$, which is analogous to the pulse controls employed in other quantum control tasks. And while the measurement frequency is large in the Zeno effect, it is still finite in practice, so it provides the feasibility of implementing this coherent control scheme in experiments.

Substituting the strength of coherent control $g = \omega\tau^{-1}$ into the Liouvillian superoperator $\mathcal{L}_{\text{tot}}^{(c)}$, the total evolution superoperator in the coherent control scheme can be simplified as

$$e^{\tau\mathcal{L}_{\text{tot}}^{(c)}(\tau)} = e^{\omega\mathcal{L}_{H_c} + (\mathcal{L}_\mu + \mathcal{L}_{H_0})\tau}. \quad (40)$$

The survival probability after a single measurement can be expanded at $\tau = 0$ as

$$p_c(\tau) = p_c(0) + \partial_\tau p_c(\tau)|_{\tau=0}\tau$$
$$+ \partial_\tau^2 p_c(\tau)|_{\tau=0}\frac{\tau^2}{2} + O(\tau^3), \quad (41)$$

where $\partial_\tau^k p_c(\tau)$ is the kth derivative of survival probability $p_c(\tau)$ at $\tau = 0$,

$$\partial_\tau^k p_c(\tau) = \langle\psi_0|\left(\partial_\tau^k e^{\tau\mathcal{L}_{\text{tot}}^{(c)}(\tau)}\right)[\rho_0]|\psi_0\rangle. \quad (42)$$

We first compute the zeroth-order term in the Taylor expansion of $p_c(\tau)$ (41),

$$p_c|_{\tau=0} = \langle\psi_0|e^{\omega\mathcal{L}_{H_c}}[\rho_0]|\psi_0\rangle. \quad (43)$$

By the definition of $\mathcal{L}_{H_c}$, $\mathcal{L}_{H_c}[\cdot] = -i[H_c, \cdot]$, $p_c|_{\tau=0}$ can be written as

$$p_c|_{\tau=0} = |\langle\psi_0|e^{-i\omega H_c}|\psi_0\rangle|^2. \quad (44)$$

To ensure that the zeroth-order term of $p_c|_{\tau=0}$ remains 1 for an arbitrary initial state $|\psi_0\rangle$, $e^{-i\omega H_c}$ needs to satisfy

$$e^{-i\omega H_c} = e^{i\theta}I, \quad (45)$$

where $e^{i\theta}$ is an arbitrary phase and I is the identity operator. This requires that

$$\omega\left(E_i^{(\mathrm{c})} - E_j^{(\mathrm{c})}\right) = 2n\pi, \quad n = \pm 1, \pm 2, \ldots, \ \forall i \neq j, \quad (46)$$

where $E_i^{(\mathrm{c})}$ and $E_j^{(\mathrm{c})}$ are two arbitrary eigenvalues of the control Hamiltonian H_c, which immediately leads to a necessary condition for the control Hamiltonian to preserve the initial state in the limit $\tau \to 0$,

$$\Delta E_{ij}^{(\mathrm{c})} / \Delta E_{i'j'}^{(\mathrm{c})} \in \mathbb{Q}, \quad \forall i \neq j, \quad i' \neq j', \quad (47)$$

where $\Delta E_{ij}^{(\mathrm{c})} = E_i^{(\mathrm{c})} - E_j^{(\mathrm{c})}$ and $\mathbb{Q}$ is the set of all rational numbers. When this condition is satisfied, $e^{\omega\mathcal{L}_{H_c}}$ can be simplified to

$$e^{\omega\mathcal{L}_{H_c}} = \mathcal{I}, \quad (48)$$

where $\mathcal{I}$ is the identity superoperator in the Liouville space.

Back to the derivatives of the evolution superoperator $e^{\mathcal{L}_{\mathrm{tot}}^{(\mathrm{c})}\tau}$, by substituting Eqs. (39) and (48) into Eq. (34), the first-order derivative of $e^{\tau\mathcal{L}_{\mathrm{tot}}^{(\mathrm{c})}(\tau)}$ at $\tau = 0$ can be rewritten as

$$\partial_\tau e^{\tau\mathcal{L}_{\mathrm{tot}}^{(\mathrm{c})}(\tau)}\big|_{\tau=0} = \int_0^1 e^{-\omega\mathcal{L}_{H_c}\eta}\left(\mathcal{L}_\mu + \mathcal{L}_{H_0}\right)e^{\omega\mathcal{L}_{H_c}\eta}\, d\eta, \quad (49)$$

and the second-order derivative of $e^{\tau\mathcal{L}_{\mathrm{tot}}^{(\mathrm{c})}(\tau)}$ can also be obtained,

$$\partial_\tau^2 e^{\tau\mathcal{L}_{\mathrm{tot}}^{(\mathrm{c})}(\tau)}\big|_{\tau=0}$$
$$= \int_0^1 d\eta_2 \int_0^{\eta_2} e^{-\omega\mathcal{L}_{H_c}\eta_2}\left(\mathcal{L}_\mu + \mathcal{L}_{H_0}\right)e^{\omega\mathcal{L}_{H_c}(\eta_2-\eta_1)}$$
$$\times \left(\mathcal{L}_\mu + \mathcal{L}_{H_0}\right)e^{\omega\mathcal{L}_{H_c}\eta_1}\, d\eta_1, \quad (50)$$

which will be useful in deriving the condition for the frequency of the measurements below.

It can be straightforwardly verified that

$$e^{-\omega\mathcal{L}_{H_c}\eta}\mathcal{L}_{H_0}e^{\omega\mathcal{L}_{H_c}\eta} = \widetilde{\mathcal{L}}_{H_0}^{(\eta)} = \mathcal{L}_{\widetilde{H}_0(\eta)},$$
$$e^{-\omega\mathcal{L}_{H_c}\eta}\mathcal{L}_\mu e^{\omega\mathcal{L}_{H_c}\eta} = \widetilde{\mathcal{L}}_\mu^{(\eta)} = \sum_k \mu_k \mathcal{D}[\widetilde{V}_k(\eta)], \quad (51)$$

where

$$\widetilde{H}_0(\eta) = e^{i\omega H_c\eta}H_0 e^{-i\omega H_c\eta},$$
$$\widetilde{V}_k(\eta) = e^{i\omega H_c\eta}V_k e^{-i\omega H_c\eta}. \quad (52)$$

The derivation of the above representation transformations of the superoperators $\mathcal{L}_{H_0}$ and $\mathcal{L}_\mu$ in the Liouville space is presented in Appendix A. So the first- and second-order derivatives of $e^{\mathcal{L}_c\tau}$ can be simplified as

$$\partial_\tau e^{\tau\mathcal{L}_{\mathrm{tot}}^{(\mathrm{c})}(\tau)}\big|_{\tau=0} = \int_0^1 \left(\widetilde{\mathcal{L}}_{H_0}^{(\eta)} + \widetilde{\mathcal{L}}_\mu^{(\eta)}\right) d\eta, \quad (53)$$

$$\partial_\tau^2 e^{\tau\mathcal{L}_{\mathrm{tot}}^{(\mathrm{c})}(\tau)}\big|_{\tau=0} = \int_0^1 d\eta_2 \int_0^{\eta_2} \left(\widetilde{\mathcal{L}}_{H_0}^{(\eta_2)} + \widetilde{\mathcal{L}}_\mu^{(\eta_2)}\right)$$
$$\times \left(\widetilde{\mathcal{L}}_{H_0}^{(\eta_1)} + \widetilde{\mathcal{L}}_\mu^{(\eta_1)}\right) d\eta_1. \quad (54)$$

The first-order derivative of survival probability (42) can then be derived by substituting Eq. (53) into (42) with $k = 1$,

$$\partial_\tau p_{\mathrm{c}}(\tau)\big|_{\tau=0} = \int_0^1 \langle\psi_0|\widetilde{\mathcal{L}}_\mu^{(\eta)}[\rho_0]|\psi_0\rangle\, d\eta, \quad (55)$$

where the fact that the average of a commutator over any quantum state is zero, i.e., $\langle\psi_0|\mathcal{L}_{\widetilde{H}_0(\eta)}[\rho_0]|\psi_0\rangle = 0$, has been considered. Hence, the effective decay rate of survival probability $\gamma_{\mathrm{eff}}(\tau)$ can be found by substituting Eq. (41) into (12) as

$$\gamma_{\mathrm{eff}}^{(\mathrm{c})}(\tau) = -\partial_\tau p_{\mathrm{c}}(\tau)\big|_{\tau=0}$$
$$- \tfrac{1}{2}\left\{\partial_\tau^2 p_{\mathrm{c}}(\tau) - [\partial_\tau p_{\mathrm{c}}(\tau)]^2\right\}\big|_{\tau=0}\tau + O(\tau^2). \quad (56)$$

Similarly, the second-order derivative of $p_{\mathrm{c}}(\tau)$ can be derived by Eq. (54) as

$$\partial_\tau^2 p_{\mathrm{c}}(\tau)\big|_{\tau=0} = \int_0^1 d\eta_2 \int_0^{\eta_2} \langle\psi_0|\left(\widetilde{\mathcal{L}}_{H_0}^{(\eta_2)} + \widetilde{\mathcal{L}}_\mu^{(\eta_2)}\right)$$
$$\times \left(\widetilde{\mathcal{L}}_{H_0}^{(\eta_1)} + \widetilde{\mathcal{L}}_\mu^{(\eta_1)}\right)[\rho_0]|\psi_0\rangle\, d\eta_1. \quad (57)$$

If the frequency of measurements $\nu = \tau^{-1}$ is required to be sufficiently large to drop the second- and higher-order terms in $\gamma_{\mathrm{eff}}^{(\mathrm{c})}(\tau)$, i.e., to reach the Zeno limit, the frequency of the projective measurements needs to satisfy

$$\nu \gg \left|\frac{\partial_\tau^2 p_{\mathrm{c}}(\tau) - [\partial_\tau p_{\mathrm{c}}(\tau)]^2}{2\partial_\tau p_{\mathrm{c}}(\tau)}\right|_{\tau=0}. \quad (58)$$

In this case the survival probability in the long-term evolution of time t can be written as

$$P_{\mathrm{c}}(t) \approx e^{-\gamma_{\mathrm{eff}}^{(\mathrm{c})}t}, \quad (59)$$

where $\gamma_{\mathrm{eff}}^{(\mathrm{c})}$ is the simplified effective decay rate on the condition (58),

$$\gamma_{\mathrm{eff}}^{(\mathrm{c})} = -\partial_\tau p_{\mathrm{c}}(\tau)\big|_{\tau=0} = -\int_0^1 \langle\psi_0|\widetilde{\mathcal{L}}_\mu^{(\eta)}[\rho_0]|\psi_0\rangle\, d\eta, \quad (60)$$

with $\widetilde{\mathcal{L}}_\mu^{(\eta)}$ given by Eq. (51).

Obviously, for a given initial state $|\psi_0\rangle$, different control Hamiltonians will lead to different effective decay rates $\gamma_{\mathrm{eff}}^{(\mathrm{c})}$, so it is desirable to optimize the control Hamiltonian to reach the minimum effective decay rate. To benchmark the performance of the coherent control scheme on protecting the Zeno effect, we define the following ratio to quantify the extent to which the control scheme can decrease the effective decay rate of the survival probability in the presence of noise:

$$\kappa \equiv \frac{\gamma_{\mathrm{eff}}^{(\mathrm{c})}}{\gamma_{\mathrm{eff}}^{(\mathrm{n})}}. \quad (61)$$

When the control slows the decay of the quantum state, κ is smaller than 1, and vice versa. And the smaller the ratio κ is, the better the coherent control scheme works.

Moreover, for given noise, the ensemble average fidelity F, which is the average fidelity between the initial state of the system and the final state evolved by the noisy quantum process over all possible initial states [78], can be invoked to characterize the overall performance of the coherent control scheme in lowering the effective decay rate for all possible

initial states $|\psi_0\rangle$ of the quantum system with a probability distribution $q(|\psi_0\rangle)$,

$$F(t) = \int q(|\psi_0\rangle) P_{|\psi_0\rangle}(t) d|\psi_0\rangle. \qquad (62)$$

The ensemble average fidelity $F(t)$ decreases with time t as the survival probability $P_{|\psi_0\rangle}(t)$ of each initial state $|\psi_0\rangle$ decreases exponentially with time, and the slower $F(t)$ decays with time, the better the protection effect is.

The ratio κ and the ensemble average fidelity $F(t)$ defined above will be employed in the next section to quantify the performance of the coherent control scheme for a two-level system with typical Markovian noise.

IV. COHERENT QUANTUM CONTROL SCHEME FOR TWO-LEVEL SYSTEMS

To illustrate how the influence of noise on the Zeno effect can be suppressed by coherent quantum controls, we consider a two-level quantum system as an example in this section.

We derive the detailed necessary condition for a coherent control scheme to preserve the Zeno effect of a two-level system in the presence of Markovian noise and obtain the effective decay rates of the survival probability with frequent repetitive projective measurements in both control-free and controlled scenarios. For the typical Markovian noise dephasing and amplitude damping, we find the optimal control Hamiltonians analytically and show the improvement of slowing the decay of survival probability by the coherent control scheme. Additionally, we investigate the performance of the coherent control scheme for initial states, and show the relation between the improvement of survival probability and the initial state by numerical illustrations.

A. Control-free scheme

First of all, we denote the excited state and the ground state of the two-level system, which is subject to free Hamiltonian evolution along with dissipative process, as $|1\rangle$ and $|0\rangle$, respectively. The density matrix of a two-level quantum system can generally be written as

$$\rho = (I + \boldsymbol{r} \cdot \boldsymbol{\sigma})/2, \qquad (63)$$

where $\boldsymbol{r} = (r_x, r_y, r_z)$ is called the Bloch vector with $|\boldsymbol{r}| \leqslant 1$ and $\boldsymbol{\sigma} = (\sigma_x, \sigma_y, \sigma_z)$ is the collection of the three Pauli operators as a vector. The excited and ground states $|1\rangle$ and $|0\rangle$ are the eigenstates of σ_z with eigenvalues -1 and 1, respectively.

In the Zeno effect, we start with a pure state $|\psi_0\rangle$ for the system, the density matrix of which can be denoted as

$$\rho_0 = |\psi_0\rangle\langle\psi_0| = \frac{I + \boldsymbol{r_0} \cdot \boldsymbol{\sigma}}{2}, \qquad (64)$$

where $\boldsymbol{r_0}$ must be a unit vector and can be written as

$$\boldsymbol{r_0} = (\sin\alpha\cos\beta, \sin\alpha\sin\beta, \cos\alpha). \qquad (65)$$

The specific form of the dissipative term $\mathcal{L}_\mu[\rho]$ in the master equation (17) for general Markovian noise on a single

qubit can be written as

$$\mathcal{L}_\mu[\rho] = \sum_{ij} \mu_{ij}\left(\sigma_i\rho\sigma_j - \frac{1}{2}\{\sigma_j\sigma_i, \rho\}\right), \quad i, j = x, y, z, \qquad (66)$$

where the coefficient matrix consisting of μ_{ij} as its elements,

$$(\Gamma)_{ij} = \mu_{ij}, \qquad (67)$$

needs to be positive semidefinite in order to guarantee the Markovianity of the noise.

According to Sec. III A, the effective decay rate of the final survival probability after an evolution of time t with noise (66) and frequent projective measurements in the Zeno limit could be obtained as

$$\gamma_{\text{eff}}^{(\text{n})} = -\langle\psi_0|\mathcal{L}_\mu[\rho_0]|\psi_0\rangle$$
$$= -\boldsymbol{r_0^T}\Gamma\boldsymbol{r_0} + \text{Tr}\Gamma + \boldsymbol{v}\cdot\boldsymbol{r_0}. \qquad (68)$$

$\boldsymbol{v}$ is a vector determined by the imaginary parts of the off-diagonal elements of the dissipation coefficient matrix Γ,

$$\boldsymbol{v} = 2(\text{Im}\mu_{23}, \text{Im}\mu_{31}, \text{Im}\mu_{12}), \qquad (69)$$

where Im denotes the imaginary part of a complex number. The derivation of Eq. (68) is given in Appendix C.

B. Coherent control scheme

In this subsection, we consider a two-level system undergoing a general Hamiltonian H_0 and general Markovian noise described by the dissipative term (66), and apply a control Hamiltonian gH_c with strength $g = \omega\tau^{-1}$ to suppress the influence of the noise, where $H_c = \boldsymbol{n_c}\cdot\boldsymbol{\sigma}$ and $\boldsymbol{n_c}$ is a unit vector denoted as

$$\boldsymbol{n_c} = (\sin\theta_c\cos\phi_c, \sin\theta_c\sin\phi_c, \cos\theta_c), \qquad (70)$$

which is the direction of the control Hamiltonian in the Bloch representation.

According to Sec. III, a necessary condition (46) is imposed on the control Hamiltonian gH_c to ensure the zeroth order of the survival probability $p(\tau)$ remaining 1. Specifically for a two-level quantum system, this condition turns to be

$$\omega = n\pi, \quad n = \pm1, \pm2, \ldots. \qquad (71)$$

With the specific form of the dissipative superoperator $\mathcal{L}_\mu$ for a two-level system given in Eq. (66), the effective decay rate of the survival probability after a single projective measurement with a coherent quantum control can be obtained from Eqs. (55) and (60) as

$$\gamma_{\text{eff}}^{(\text{c})} = -\partial_\tau p_c(\tau)|_{\tau=0},$$

$$= -\sum_{i,j=1}^{3}\mu_{ij}\int_0^1 \text{Tr}\left[\rho_0\widetilde{\sigma}_i^{(\eta)}\rho_0\widetilde{\sigma}_j^{(\eta)} - \rho_0\widetilde{\sigma}_j^{(\eta)}\widetilde{\sigma}_i^{(\eta)}\right]d\eta, \qquad (72)$$

where $\widetilde{\sigma}_i^{(\eta)} = e^{i\omega H_c\eta}\sigma_i e^{-i\omega H_c\eta}$ denotes the ith Pauli operator in the framework rotated by $e^{-i\omega H_c\eta}$ dependent on the parameter η.

When the necessary condition (71) is met and the measurement frequency reaches the Zeno limit, the effective decay rate

of the survival probability can be worked out by Eq. (72) as

$$
\begin{aligned}
\gamma_{\text{eff}}^{(c)} = &-\tfrac{3}{2}(\boldsymbol{n_c} \cdot \boldsymbol{r_0})^2 \boldsymbol{n_c^T} \Gamma \boldsymbol{n_c} + \tfrac{1}{2}(\boldsymbol{n_c} \cdot \boldsymbol{r_0})\big(\boldsymbol{n_c^T}\Gamma\boldsymbol{r_0} + \boldsymbol{r_0^T}\Gamma\boldsymbol{n_c}\big) \\
&- \tfrac{1}{2}\boldsymbol{r_0^T}\Gamma\boldsymbol{r_0} - \tfrac{1}{2}(\boldsymbol{n_c} \times \boldsymbol{r_0})^T\Gamma(\boldsymbol{n_c} \times \boldsymbol{r_0}) \\
&+ \text{Tr}\,\Gamma + (\boldsymbol{n_c} \cdot \boldsymbol{r_0})(\boldsymbol{v} \cdot \boldsymbol{n_c}),
\end{aligned} \tag{73}
$$

where $\boldsymbol{v}$ is the vector defined in Eq. (69) and the superscript "T" denotes the matrix transposition. The details of derivation are provided in Appendix C.

It can be observed that when $\boldsymbol{n_c} \cdot \boldsymbol{r_0} = \pm 1$, i.e., the direction of the Hamiltonian $\boldsymbol{n_c}$ is parallel or antiparallel with that of the initial state $\boldsymbol{r_0}$ since both $\boldsymbol{n_c}$ and $\boldsymbol{r_0}$ are unit vectors, the effective decay rate $\gamma_{\text{eff}}^{(c)}$ in Eq. (73) will coincide with $\gamma_{\text{eff}}^{(n)}$ without quantum control in Eq. (68), which means the coherent control does not have any effect on the decay rate in this case, leading to another necessary condition for the validity of the coherent control scheme on a two-level system,

$$
\boldsymbol{n_c} \neq \pm\boldsymbol{r_0}. \tag{74}
$$

By evaluating the ratio κ defined in Eq. (61) with the results for $\gamma_{\text{eff}}^{(n)}$ and $\gamma_{\text{eff}}^{(c)}$ in Eqs. (68) and (73), one can determine the effect of the coherent control scheme on the two-level system. In particular, if $\kappa > 1$, the decay of the survival probability accelerates, and if $\kappa < 1$, the decay slows down.

It can be observed from Eq. (73), that for given noise $\mathcal{L}_\mu$'s and an initial state ρ_0, the effective decay rate $\gamma_{\text{eff}}^{(c)}$ of a two-level system varies with different quantum control Hamiltonian H_c, so one can optimize the control Hamiltonian to minimize the decay rate of the survival probability. The optimization for the control Hamiltonian H_c can be formally solved by a variational approach, with the Lagrangian function constrained by the normalization condition $\boldsymbol{n_c} = 1$ as

$$
L(P_n, \Lambda) = \gamma_{\text{eff}}^{(c)} + \text{Tr}\big[\big(P_n^2 - P_n\big)\Lambda\big], \tag{75}
$$

where the Lagrange multiplier Λ is an arbitrary matrix and $P_n \equiv \boldsymbol{n_c}\boldsymbol{n_c^T}$ is the projection operators on to the unit vector $\boldsymbol{n_c}$ in the three-dimensional Bloch space.

To obtain the optimal control Hamiltonian to minimize the effective decay rate $\gamma_{\text{eff}}^{(c)}$ of the two-level quantum system, the variation of the Lagrangian function (75) needs always to be zero for any δP_n and $\delta\Lambda$ according to the principle of variation approach, leading to the optimization equation for the projector P_n onto the unit vector $\boldsymbol{n_c}$ along the direction of the control Hamiltonian,

$$
\begin{aligned}
&-\tfrac{3}{2}\Gamma P_n P_r - \tfrac{3}{2}P_r P_n \Gamma + \tfrac{1}{2}\Gamma P_r + \tfrac{1}{2}P_r \Gamma \\
&- \tfrac{1}{2}R^T\Gamma R + \boldsymbol{r_0}\boldsymbol{v}^T + P_n\Lambda + \Lambda P_n - \Lambda = \boldsymbol{0},
\end{aligned} \tag{76}
$$

with the constraint condition $P_n^2 = P_n$, where $P_r = \boldsymbol{r_0}\boldsymbol{r_0^T}$ is the projection operators onto the vector $\boldsymbol{r_0}$ in the Bloch space and R is an antisymmetric matrix,

$$
R = \begin{bmatrix} 0 & z_0 & -y_0 \\ -z_0 & 0 & x_0 \\ y_0 & -x_0 & 0 \end{bmatrix}, \tag{77}
$$

with $\boldsymbol{r_0} = (x_0, y_0, z_0)$. The detail of derivation is provided in Appendix B. Once the optimization Eq. (76) is solved, the direction of the optimal control Hamiltonian can be determined, and the optimal control Hamiltonian can be obtained by this direction with the leading factor given in Eq. (71).

C. Examples

To illustrate the above general theoretical results, we investigate the effect of coherent quantum controls on two-level quantum systems with two typical types of Markovian noise, the dephasing and the amplitude damping. By deriving the effective decay coefficients $\gamma_{\text{eff}}^{(n)}$ and $\gamma_{\text{eff}}^{(c)}$ under these specific noise channels, we find the optimal coherent controls tailored for different initial states of two-level quantum systems. Furthermore, we devote to unveiling the physical pictures underlying the optimal coherent control strategy for each type of noise. Through a comparative analysis of the decay rate and the ensemble average fidelity between the cases with or without the optimal coherent control in the presence of noise, we demonstrate the advantage of this coherent control scheme in protecting the Zeno effect both analytically and numerically.

In addition, we will also consider the impact of different initial states of the quantum system the improvement of the effective decay rates brought by the coherent quantum controls, and study the relation between the initial state and the extent to which the decay rate can be decreased by coherent control in detail through numerical computation.

1. Dephasing

The dephasing noise is a typical unitary noise described by a dissipative term $\mathcal{D}[\sigma_z]$ in a quantum master equation, and has been extensively studied in the theory of open quantum systems, with the noise coefficient matrix (67) as

$$
\Gamma_z = \begin{pmatrix} 0 & 0 & 0 \\ 0 & 0 & 0 \\ 0 & 0 & \mu \end{pmatrix}. \tag{78}
$$

The evolution of a two-level quantum system under a free Hamiltonian H_0 and the dephasing noise with an intensity μ is determined by the master equation

$$
\frac{d\rho_t}{dt} = -i[H_0, \rho_t] + \mu\mathcal{D}[\sigma_z]\rho_t, \tag{79}
$$

where $\mathcal{D}[\sigma_z]\rho_t = \sigma_z\rho_t\sigma_z - \rho_t$ and ρ_t is the density matrix of the system at time t. When a control Hamiltonian gH_c is introduced to the system, the master equation becomes

$$
\frac{d\rho_t}{dt} = -i[H_0 + gH_c, \rho_t] + \mu\mathcal{D}[\sigma_z]\rho_t. \tag{80}
$$

The effect of the dephasing noise on a two-level system is plotted in Fig. 2. It shows that the Bloch sphere, which includes all possible density matrices of a two-level system, is "compressed" towards the z axis by the dephasing noise. And the compression is symmetric about the equatorial plane as the dephasing noise does not change the σ_z component of any density matrix and rotationally symmetric around the z axis as the dephasing noise affects the σ_x and σ_y components of all density matrices uniformly.

When the frequency of the projective measurement is large enough and the condition (71) is satisfied in the Zeno limit $\tau \to 0$, by substituting the $\boldsymbol{r_0}$ (65) and Γ_z (78) into the Eqs. (68) and (73), one can obtain the effective decay rates of survival probability without the coherent control,

$$
\gamma_{\text{eff}}^{(n)} = \frac{\mu}{2}(1 - \cos 2\alpha), \tag{81}
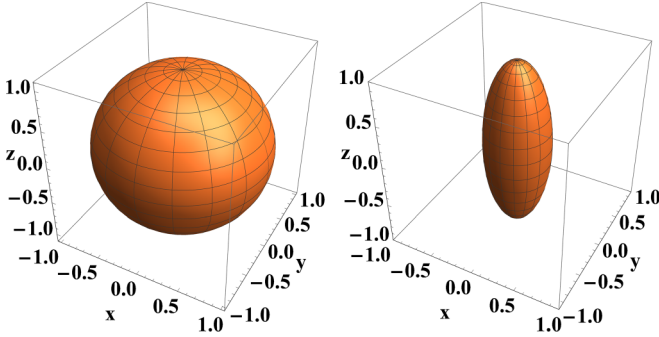$$

FIG. 2. Transformation of the Bloch sphere under the dephasing noise. The dephasing noise results in the invariance of z components of the Bloch vectors and uniform contraction of the x and y towards the z axis. Parameter: $\mu t = 1/2$.

and with the coherent control,

$$
\begin{aligned}
\gamma_{\text{eff}}^{(c)} = \frac{\mu}{64}[&39 - 2\cos 2\alpha(1 + 3\cos 2\theta_c)^2 \\
&- 3\cos 4\theta_c - 8\cos 2\Delta \sin^2 \alpha \sin^2 \theta_c \\
&- 4\cos 2\theta_c(1 + 6\cos 2\Delta \sin^2 \alpha \sin^2 \theta_c) \\
&- 4\cos \Delta \sin 2\alpha(2\sin 2\theta_c + 3\sin 4\theta_c)], \quad (82)
\end{aligned}
$$

where $\Delta = \beta - \phi_c$.

From the result of $\gamma_{\text{eff}}^{(n)}$ (81), it is evident that the decay rate of survival probability induced by the dephasing noise is independent of the azimuthal angle β and solely dependent on the polar angle α between the initial state and the z axis, and is symmetric about $\alpha = \pi/2$, in agreement with the symmetries of the impact of the dephasing noise on the Bloch sphere shown in Fig. 2. When the angle α is zero or π, the initial state remains unaffected by the noise as it lies along the compression axis, i.e., the z axis, so no decay occurs in the survival probability in this case. However, when the polar angle α is $\pi/2$, the effect of noise becomes maximal, and the effective decay rate increases to $\mu/2$. An intriguing discovery emerges from Eq. (82): the ratio $\kappa = \gamma_{\text{eff}}^{(c)}/\gamma_{\text{eff}}^{(n)}$ with the coherent control optimized is independent of the noise intensity μ, suggesting the coherent control scheme is robust against different strengths of the dephasing noise, which is a desirable property for application of this control scheme in real environments.

Due to the different impacts of the dephasing noise on different initial states of the two-level system, the extent to which the decay of the survival probability can be decreased by coherent quantum controls is also different. Obviously, when the Bloch vector of the initial state lies along the z axis, i.e., $\alpha = 0, \pi$, the dephasing noise does not change the initial state, so any coherent quantum control cannot improve the probability for the system to stay in the initial state if it does not even worsen the decay of survival probability. Note that the free Hamiltonian may rotate the initial state from the z axis to another direction that suffers from the dephasing noise, but as repetitive projective measurements are performed on the system with a sufficiently large frequency, the change of the system induced by the free Hamiltonian is much slower than the Zeno effect induced by the frequent projective measurements. So in the Zeno limit $\tau \to 0$, the

impact of the free Hamiltonian on the decay of the survival probability can be neglected. This is also the reason why the free Hamiltonian does not appear in the effective decay rate of survival probability (82).

On the contrary, when the Bloch vector of the initial state stays on the equator of the Bloch sphere, i.e., $\alpha = \pi/2$, the impact of the dephasing noise is most significant and the probability for the system to survive in the initial state is worst. In this case, any Bloch vector other than those on the equator can suffer less from the dephasing noise, so any coherent quantum control can improve the survival probability of the system in the presence of dephasing noise though the improvement can differ by different control Hamiltonians. And, similar as above, the impact of the free Hamiltonian is negligible as we are considering the Zeno limit here.

The initial states along the z axis and on the equator of the Bloch sphere are the two limiting cases regarding the influence of the dephasing noise on the survival probability and the extent to which coherent quantum controls may help. For any other intermediate cases, the initial states can suffer from the dephasing noise but not as much as those on the equator of the Bloch sphere, and accordingly coherent quantum controls can improve the survival probability of system to stay in the initial states but not as much as for the initial states on the equator. And actually coherent quantum controls may even worsen the survival probability if the control Hamiltonian is not chosen properly in this case.

To gain an intuitive picture of how different choices of the initial state affect the impact of the dephasing noise and the extent that coherent quantum controls can improve the survival probability, the effective decay rates of the survival probability in the above three cases are depicted in Fig. 3 for three typical initial states,

$$
\begin{aligned}
|\psi_a\rangle &= |0\rangle, \\
|\psi_b\rangle &= \frac{1}{\sqrt{2}}(|0\rangle + |1\rangle), \quad (83) \\
|\psi_c\rangle &= \cos\frac{\pi}{8}|0\rangle + \sin\frac{\pi}{8}|1\rangle,
\end{aligned}
$$

which belong to the three different cases respectively.

Figures 3(a1) and 3(a2) depict the effective decay rate for the initial state $|\psi_a\rangle$ with $\alpha = 0$, lying along the z axis of the Bloch sphere. It can be seen that $\gamma_{\text{eff}}^{(c)} \geqslant \gamma_{\text{eff}}^{(n)}$, i.e., any coherent control can only induce the decay of survival probability or keep it unchanged at most, since the initial state is already in the most favorable direction which is free from the impact of dephasing, and any coherent control scheme may not reduce the decay in this case. As a contrast, Figs. 3(b1) and 3(b2) depict the decay rate for the initial state $|\psi_b\rangle$ with $\alpha = \pi/2, \beta = 0$, lying on the equator of the Bloch sphere. It can be seen from the figure that $\gamma_{\text{eff}}^{(c)} \leqslant \gamma_{\text{eff}}^{(n)}$, i.e., any control Hamiltonian can improve the survival probability or keep it unchanged at least, since the initial state experiences the most severe impact of the dephasing noise, and thus any coherent control scheme cannot do worse than without the control. Figures 3(c1) and 3(c2) depict the intermediate case for the initial state $|\psi_c\rangle$ with $\alpha = \pi/4, \beta = 0$, lying along a direction between the z axis and the equator of the Bloch sphere. It can be observed that some choices of the control Hamiltonian can improve the decay of survival probability while the others may
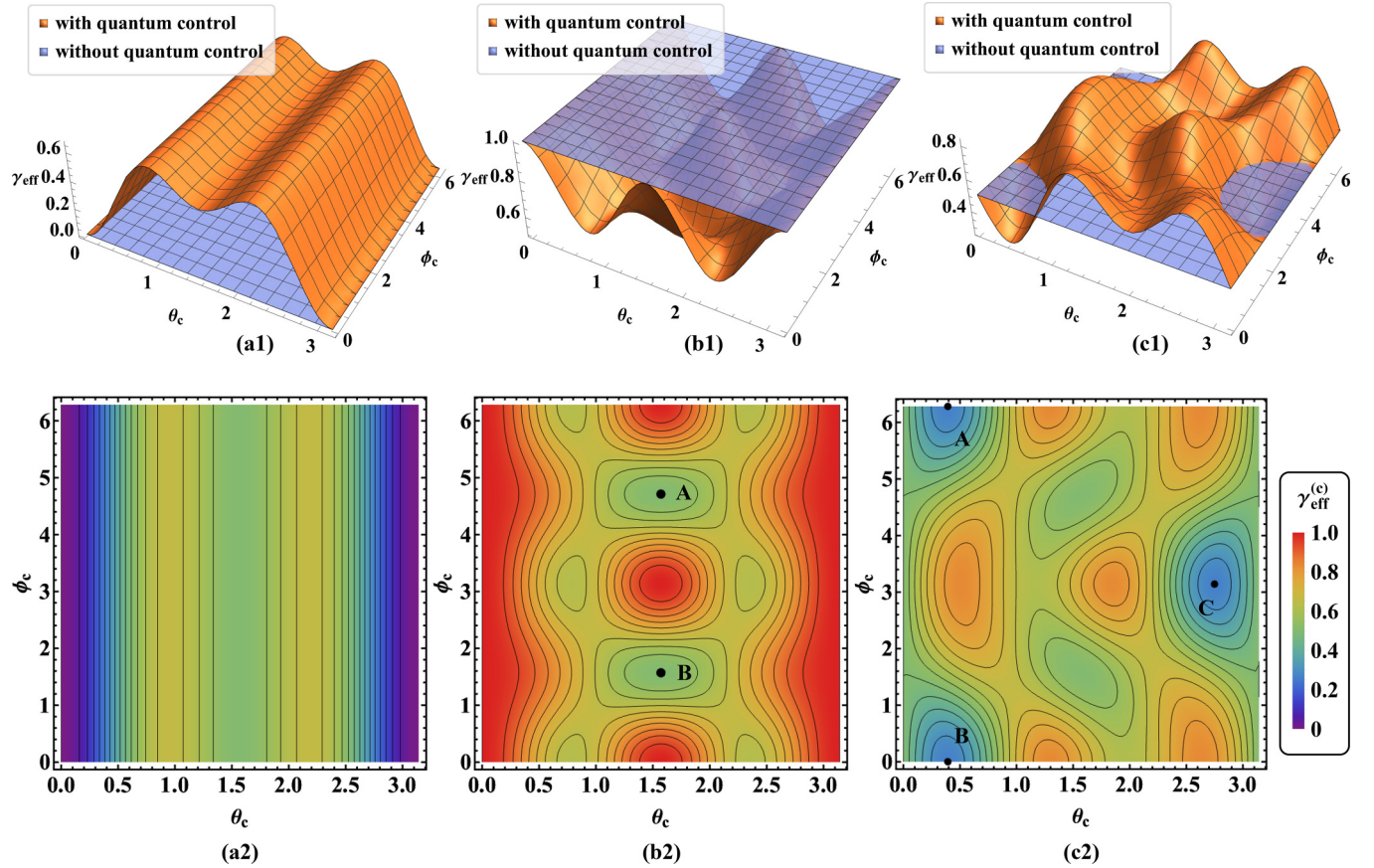
FIG. 3. Illustration of effective decay rate γ_{eff} for different initial states: (a) $\alpha_{\mathrm{a}} = 0$, (b) $\alpha_{\mathrm{b}} = \pi/2$, and (c) $\alpha_{\mathrm{c}} = \pi/4$, with and without quantum control against dephasing noise. The decay rate $\gamma_{\mathrm{eff}}^{(\mathrm{n})}$ without the coherent control is plotted by the blue surface, and the decay rate $\gamma_{\mathrm{eff}}^{(\mathrm{c})}$ with the coherent control is plotted by the orange surface. When the initial state is $\alpha = 0$, the direction of the optimal quantum control is parallel to that of the initial state $\theta_{\mathrm{c}} = 0$ or π, which is a trivial control. When the initial state is $\alpha = \pi/2$, the directions for the most optimal controls can be obtained as $\{\theta_{\mathrm{c}} = \pi/2, \phi_{\mathrm{c}} = \pi/2, 3\pi/2\}$, the effective decay rates under which are indicated by points A and B in subfigure (b2). When the initial state is $\alpha = \pi/4$, the optimal controls can be found as $\{\theta_{\mathrm{c}} = \pi/8, \phi_{\mathrm{c}} = 0; \theta_{\mathrm{c}} = 7\pi/8, \phi_{\mathrm{c}} = \pi\}$ and effective decay rate is indicated by the three annotated points A, B, and C in subfigure (c2). Parameters: $\beta = 0$, $\omega = \pi$, and $\mu = 1$.

worsen it, as there exist both directions that suffer more or less from the dephasing noise on the Bloch sphere and the control Hamiltonian may rotate the system to either of them in this case. As shown by Fig. 3, different directions of the control Hamiltonian have different capabilities to improve the survival probability given the initial state of the system, so in the following our objective is to find the optimal direction of the control Hamiltonian that minimizes the effective decay rate $\gamma_{\mathrm{eff}}^{(\mathrm{c})}$ to protect the Zeno effect.

According to the general variation Eq. (76) for a two-level system along with the positive definiteness of the Hessian matrix [79] for $\gamma_{\mathrm{eff}}^{(\mathrm{opt})}$ with respect to direction parameters θ_{c} and ϕ_{c} of the control Hamiltonian to ensure the minimization (not the maximization) of the decay rate $\gamma_{\mathrm{eff}}^{(\mathrm{c})}$, we have the following optimization equations for θ_{c} and ϕ_{c}:

$$\partial_{\theta_{\mathrm{c}}} \gamma_{\mathrm{eff}}^{(\mathrm{c})} = 0,$$
$$\partial_{\phi_{\mathrm{c}}} \gamma_{\mathrm{eff}}^{(\mathrm{c})} = 0,$$
$$A > 0, \ C > 0, \qquad\qquad (84)$$
$$AC - B^2 < 0,$$

where $A = \partial_{\theta_{\mathrm{c}}}^2 \gamma_{\mathrm{eff}}^{(\mathrm{c})}$, $C = \partial_{\phi_{\mathrm{c}}}^2 \gamma_{\mathrm{eff}}^{(\mathrm{c})}$, and $B \equiv \partial_{\theta_{\mathrm{c}}} \partial_{\phi_{\mathrm{c}}} \gamma_{\mathrm{eff}}^{(\mathrm{c})}$.

One can obtain the optimal directions of the control Hamiltonian in the presence of dephasing noise given the Bloch vector $\boldsymbol{r_0}$ of the initial state of the two-level quantum system by solving Eq. (84),

$$
\begin{aligned}
\theta_{\mathrm{c}} &= \tfrac{\alpha}{2}, \phi_{\mathrm{c}} = \beta, & \arccos\left(\tfrac{1}{3}\right) < \alpha \leqslant \pi, \\
\theta_{\mathrm{c}} &= \tfrac{\pi+\alpha}{2}, \phi_{\mathrm{c}} = \beta, & 0 \leqslant \alpha < \arccos\left(-\tfrac{1}{3}\right), \\
\theta_{\mathrm{c}} &= \tfrac{\pi}{2}, \phi_{\mathrm{c}} = \beta + \tfrac{\pi}{2}.
\end{aligned}
\qquad (85)
$$

Note that the solutions in Eq. (85) include all the local optimal points for the direction of the control Hamiltonian. To find the global optimal point for the control Hamiltonian, one needs to substitute this solution into the effective decay rate $\gamma_{\mathrm{eff}}^{(\mathrm{c})}$ (82) and compare the results corresponding to the three scenarios in Eq. (85). The global minimum effective decay rate turns out to be

$$
\gamma_{\mathrm{eff}}^{(\mathrm{opt})} =
\begin{cases}
-\frac{\mu}{16}(-7 + 4\cos\alpha + 3\cos 2\alpha), & 0 \leqslant \alpha < \alpha_0, \\
\frac{\mu}{2}, & \alpha_0 \leqslant \alpha < \alpha_1, \\
-\frac{\mu}{4}\cos^2\alpha(-5 + 3\cos\alpha), & \alpha_1 \leqslant \alpha \leqslant \pi,
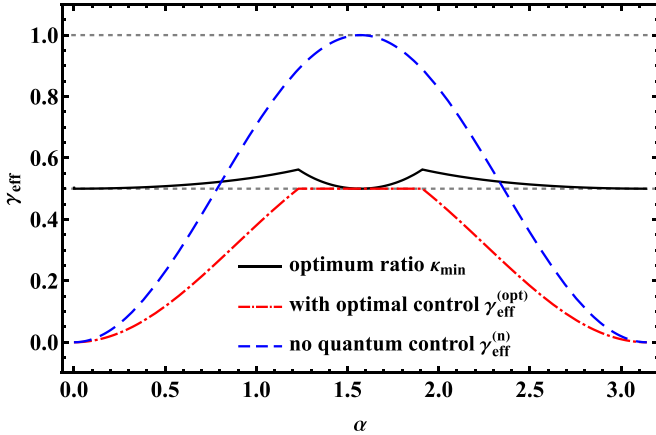\end{cases}
\qquad (86)
$$

FIG. 4. Illustration of effective decay rates of the survival probability with or without the coherent control in the presence of dephasing noise for different initial states. The decay rate $\gamma_{\text{eff}}^{(\text{n})}$ without the coherent control is plotted by the blue dashed line, and the minimum decay rate $\gamma_{\text{eff}}^{(\text{opt})}$ with the optimized coherent control is plotted by the red dot-dashed line. The ratio $\kappa_{\min} = \gamma_{\text{eff}}^{(\text{opt})}/\gamma_{\text{eff}}^{(\text{n})}$ is also plotted by the black solid line, which shows the stability of the optimization performance of this coherent control scheme over different initial states of the system. Parameters: $\omega = \pi$ and $\mu = 1$.

where $\alpha_0 \equiv 2\arccos\sqrt{2}$, $\alpha_1 = \pi - \alpha_0$ and μ is the noise strength introduced in the master Eq. (80).

It can be observed that the optimal effective decay rate $\gamma_{\text{eff}}^{(\text{opt})}$ with the coherent quantum control and the decay rate $\gamma_{\text{eff}}^{(\text{n})}$ without any control are both independent of the azimuthal angle β of the Bloch vector of the initial state. This characteristic arises from the rotational symmetry of dephasing noise about the z axis.

The relations between the decay rates $\gamma_{\text{eff}}^{(\text{opt})}$, $\gamma_{\text{eff}}^{(\text{n})}$ and the polar angle α of the Bloch vector of the initial state as well as the optimal ratio κ for different initial states are depicted in Fig. 4. In the figure, one can observe that the optimized effective decay rate $\gamma_{\text{eff}}^{(\text{opt})}$ always remains lower than the decay rate without control $\gamma_{\text{eff}}^{(\text{n})}$, indicating the effectiveness of the coherent control scheme. It can also be observed from the figure that the coherent control scheme is robust against the change of the polar angle α as the optimized ratio κ has only minor fluctuation over the whole range of α, achieving the minimum value $1/2$ near the poles ($\alpha = 0$ or π) of the Bloch sphere where the influence of the dephasing noise is negligible and on the equator ($\alpha = \pi/2$) where the influence of the dephasing noise is most significant. The optimization performance is poorest at $\alpha = \alpha_0$ and $\pi - \alpha_0$, where $\kappa = 9/16$. So the ratio κ changes only slightly over the range of α.

To characterize the overall performance of the above optimized coherent quantum control scheme over different initial states of the system, we consider the ensemble average fidelity F (62) over uniformly distributed initial states, which turns out to be

$$F(t) = \frac{1}{4\pi} \int_0^{2\pi} d\beta \int_0^\pi d\alpha\, e^{-\gamma_{\text{eff}}t} \sin\alpha, \qquad (87)$$

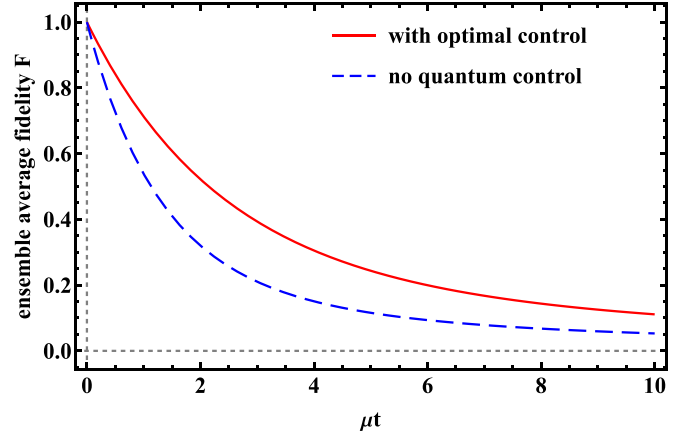for a two-level system. The spherical integral is due to the distribution of initial states on the Bloch sphere

FIG. 5. Plots of the ensemble average fidelity F with respect to μt in the presence of dephasing noise with the optimal coherent control scheme and without any quantum control, respectively.

with a radius $|\boldsymbol{r_0}| = 1$, and $\frac{1}{4\pi}$ is the normalization coefficient.

By substituting Eqs. (81) and (86) into (87), one can obtain the decay of the ensemble average fidelity F with respect to μt in both the control-free and optimally controlled cases, as shown in Fig. 5. It is evident from the figure that the ensemble average fidelity F with the optimal coherent control is always greater than that in the control-free scenario, indicating a slower decay of the survival probability with the optimal coherent control given the same noise intensity μ. This observation explicitly demonstrates the effectiveness of the above coherent quantum control strategy in protecting the quantum Zeno effect against the dephasing noise.

It is helpful to pause and ponder the physical mechanism behind the optimization effect of the above coherent control scheme. For the dephasing noise, the z axis is the direction that is not disturbed by the noise, so it would be beneficial to rotate a quantum state towards the z axis during the evolution by quantum control to reduce the influence of the dephasing noise. As the Hamiltonian control is a coherent control scheme which preserves the purity of a quantum system, one actually wants to rotate the quantum system towards the $|0\rangle$ or $|1\rangle$ state, i.e., the north or south pole of the Bloch sphere.

This is indeed what the above Hamiltonian control scheme does, as illustrated by Fig. 6. From the three colored lines in Fig. 6 which represent the evolution paths of the quantum system with the optimal control Hamiltonians, it can be seen that the Hamiltonian control drags the quantum system towards the $|0\rangle$ state (as the initial state is chosen to be in the upper hemisphere in the figure, which is closer to $|0\rangle$) and then turns it back to the vicinity of the initial state (as the purpose is to preserve the initial state), which is the physical significance of the condition (71). The joint effect of the Hamiltonian control and the dephasing noise is to approximately rotate the state of quantum system between the initial state and the north/south pole of Bloch sphere along a spiral path towards the z axis, realizing the decrease of decay caused by the dephasing noise. As a contrast, the quantum system evolves along the black paths without quantum control which decays to the z axis faster.

(a) $\alpha = \alpha_0, \beta = 0.$　　　　(b) $\alpha = \pi - \alpha_0, \beta = 0.$　　　　(c) $\alpha = \pi, \beta = 0.$
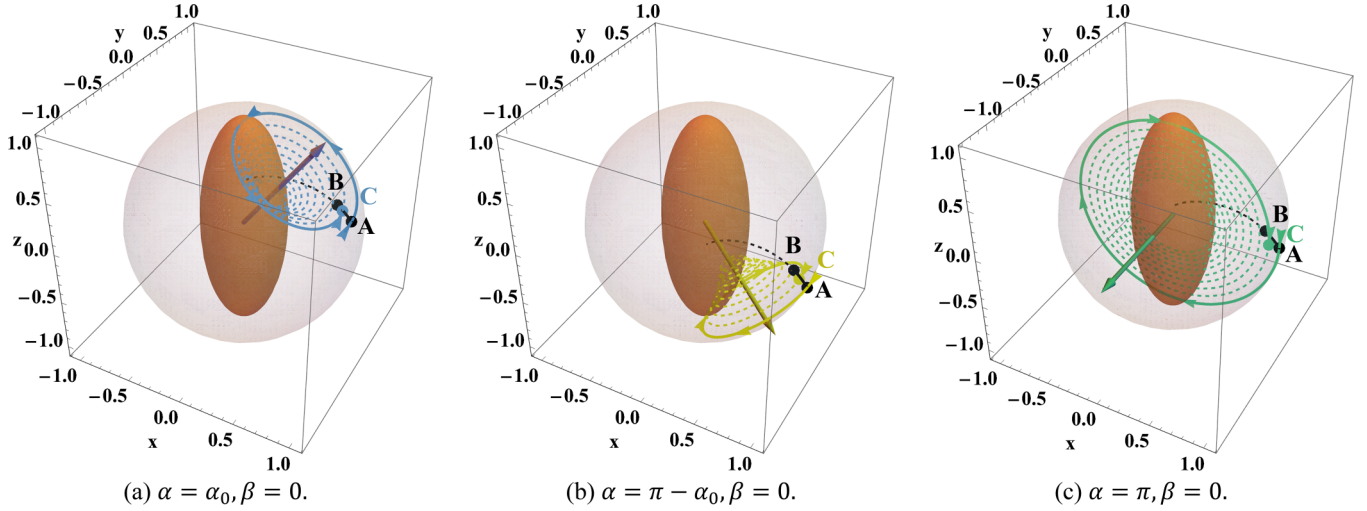
FIG. 6. Illustration for the evolution paths of a two-level quantum system initially prepared on different pure states with and without the protection by the optimal coherent control between two consecutive projective measurements in the presence of dephasing noise. In each subfigure, the gray, translucent sphere is the Bloch sphere consisting of all density matrices of a single qubit, the orange, translucent ellipsoid is the set of all density matrices after the disturbance of the dephasing noise on the system, and the arrow indicates the direction of optimal control Hamiltonian. Point A represents the initial state, and points B and C represent the final states at the end of each time interval without and with the Hamiltonian control, respectively. The black lines depict the evolution paths of the system without quantum controls, whereas the colored lines represent the evolution paths engineered by the optimal controls. The solid arcs of the colored lines depict the actual evolution paths between two consecutive projective measurements, while the dashed arcs of the colored lines depict the following evolution paths if the evolution is not interrupted by the projective measurement. Typical initial states of the quantum system are chosen for the three different regimes given by Eq. (86), respectively: (a) $\alpha \leqslant \alpha_0$ (b) $\alpha \geqslant 1 - \alpha_0$, and (c) $\alpha_0 < \alpha < 1 - \alpha_0$. Parameters: $H_0 = \sigma_z$, $\beta = 0$, $\mu = 1$, $\omega = \pi$, $\tau = 0.01$.

It is worth noting that the system cannot perfectly return to the initial state at the end of each cycle in spite of the Hamiltonian control, due to the existence of nonzero first-order term in the survival probability which can be lowered by the coherent control scheme but not eliminated. But it can be seen from Fig. 6 that the distance between the initial state (point A) and the final state with the quantum control (point C) is always shorter than that between the initial state and the final state without the quantum control (point B), indicating the effectiveness of the above quantum control scheme.

It is also worth mentioning that while the unitary noise considered in this subsection is the dephasing noise, the above optimal control scheme can be generalized for arbitrary unitary noise, since the effect of a unitary noise other than the dephasing is equivalent to a new free Hamiltonian with the dephasing noise in a rotated picture, which can be included above due to the arbitrariness of free Hamiltonian assumed in the above study.

2. Amplitude damping

The amplitude damping is another typical noise on a two-level system, usually describing the energy loss from a quantum system, known as energy dissipation. The noise coefficient matrix (67) of amplitude damping is

$$\Gamma_{\rm ad} = \frac{\mu}{4}\begin{pmatrix} 1 & -i & 0 \\ i & 1 & 0 \\ 0 & 0 & 0 \end{pmatrix}, \tag{88}$$

and the master equation for the evolution of the system with a free Hamiltonian and the amplitude damping

noise is

$$\frac{d\rho_t}{dt} = -i[H_0, \rho_t] + \mu\mathcal{D}[\sigma_-]\rho_t, \tag{89}$$

where $\mathcal{D}[\sigma_-]\rho_t = \sigma_-\rho_t\sigma_+ - \frac{1}{2}\{\sigma_+\sigma_-, \rho_t\}$ and ρ_t is the density matrix of the system at time t. When a control Hamiltonian $gH_{\rm c}$ is applied on the system, the master equation becomes

$$\frac{d\rho_t}{dt} = -i[H_0 + gH_{\rm c}, \rho_t] + \mu\mathcal{D}[\sigma_-]\rho_t. \tag{90}$$

The effect of the amplitude damping noise on a two-level system is depicted in Fig. 7. It shows that the amplitude damping noise compresses the Bloch sphere towards the north pole, i.e., the state $|0\rangle$ which is the unique stationary state of
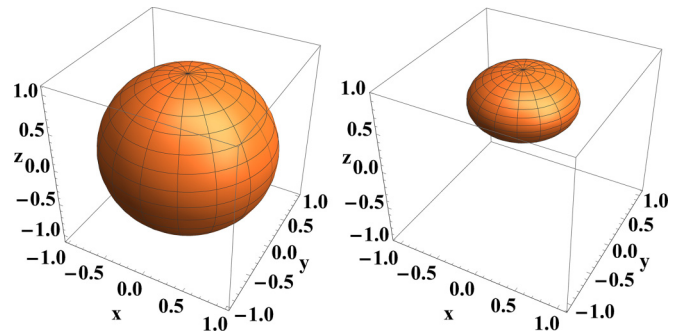

FIG. 7. Effect of the amplitude damping noise on a two-level system. The amplitude damping noise compresses the Bloch sphere towards the north pole, i.e., the quantum state $|0\rangle$, which is the stationary state of the amplitude damping noise. Parameter: $\mu t = 1$.

the amplitude damping noise. The compression is rotationally symmetric around the z axis as the amplitude damping noise affects the σ_x and σ_y components of all density matrices uniformly, but in contrast to the dephasing noise discussed above, it is not symmetric about the equatorial plane as the amplitude damping noise also changes the σ_z component of a density matrix, and this change varies with the σ_z component of the density matrix.

When the projective measurement is performed sufficiently frequently and the condition (71) to preserve the initial state is satisfied in the Zeno limit $\tau \to 0$, by substituting $\boldsymbol{r_0}$ (71) and Γ_{ad} (88) into the Eqs. (68) and (73), one can obtain the effective decay rate of survival probability without the Hamiltonian control as

$$\gamma_{\mathrm{eff}}^{(\mathrm{n})} = \frac{\mu}{8}(3 - 4\cos\alpha + \cos 2\alpha) = \mu\sin^4\frac{\alpha}{2}, \qquad (91)$$

and the effective decay rate with the control Hamiltonian as

$$
\begin{aligned}
\gamma_{\mathrm{eff}}^{(\mathrm{c})} = \frac{\mu}{512}\{&178 + 12\cos 2(\alpha - \theta_{\mathrm{c}}) + \cos 2(\alpha - \Delta) \\
&+ \cos 2(\alpha + \Delta) - 256\cos\alpha\cos^2\theta_{\mathrm{c}} + 8\cos 2\theta_{\mathrm{c}} \\
&+ 6\cos 4\theta_{\mathrm{c}} + 2\cos 2\alpha(11 + 6\cos 2\theta_{\mathrm{c}} + 9\cos 4\theta_{\mathrm{c}}) \\
&+ 2\cos 2\Delta(-1 + 2(4\cos 2\theta_{\mathrm{c}} - 3\cos 4\theta_{\mathrm{c}})\sin^2\alpha) \\
&+ 4[-32\cos\Delta\sin\alpha + (4\cos\Delta(1 + 3\cos 2\theta_{\mathrm{c}}) \\
&- 3)\sin 2\alpha]\sin 2\theta_{\mathrm{c}}\},
\end{aligned}
\qquad (92)
$$

where $\Delta = \beta - \phi_{\mathrm{c}}$.

From the result of $\gamma_{\mathrm{eff}}^{(\mathrm{n})}$ (91) without Hamiltonian control, it's apparent that the decay rate of the survival probability induced by the amplitude damping noise is independent of the azimuthal angle β and solely depends on the polar angle α between the initial state and the z axis. This is in accordance with the rotational symmetry of the compression effect of the amplitude damping noise around the z axis shown in Fig. 7. However, an additional term, $\cos\alpha$, is introduced in $\gamma_{\mathrm{eff}}^{(\mathrm{n})}$ (91), which is not symmetric about $\alpha = \pi/2$, so the decay rate is not symmetric about the equatorial plane and the decay increases with α, which also agrees with Fig. 7. The north pole of the Bloch sphere, i.e., the state $|0\rangle$, is a stationary state of the amplitude damping noise, so it remains unaffected by the amplitude damping noise, and no decay of the survival probability occurs when the system is initially in this state. On the contrary, the south pole of the Bloch sphere, i.e., the state $|1\rangle$, is the state whose Bloch vector is compressed most by the amplitude damping noise, so when the initial state of the system resides at the south pole, the survival probability decays most significantly with time.

When coherent quantum control is applied on the system, similar as the dephasing noise discussed above, the impact of the amplitude damping noise differs with the initial state of the two-level system. When the initial state of the system is $|0\rangle$, i.e., $\alpha = 0$, the north pole of the Bloch sphere, the amplitude damping noise does not change the system as $|0\rangle$ is the stationary state of the amplitude damping noise and the survival probability does not decay. So applying any control Hamiltonian on the system can only induce decay on the survival probability. On the contrary, when the system is initially in the state $|1\rangle$, i.e., $\alpha = \pi$, the south pole of the Bloch sphere,

the system suffers the most disturbance from the amplitude damping noise and the survival probability decays fastest. So in this case, introducing any control Hamiltonian to the system can help slow the decay of survival probability. When the system initially stays at any state other than $|0\rangle$ or $|1\rangle$, a control Hamiltonian may decrease or increase the decay rate of the survival probability, as one can always find another state that is better or worse than the initial state in suffering the amplitude damping noise, which is an intermediate case between the states $|0\rangle$ and $|1\rangle$.

To visualize the effects of the Hamiltonian controls on different initial states of the system in the presence of amplitude damping noise, the effective decay rate of the survival probability $\gamma_{\mathrm{eff}}^{(\mathrm{c})}$ (92) with all possible directions of the control Hamiltonian is plotted in Fig. 8 for three typical initial states of the system,

$$
\begin{aligned}
|\psi_{\mathrm{a}}\rangle &= |0\rangle, \\
|\psi_{\mathrm{b}}\rangle &= |1\rangle, \\
|\psi_{\mathrm{c}}\rangle &= \frac{1}{\sqrt{2}}(|0\rangle + |1\rangle),
\end{aligned}
\qquad (93)
$$

which falls into the three different categories of the states discussed above respectively.

Figures 8(a1) and 8(b1) depict the effective decay rate for the state $|\psi_{\mathrm{a}}\rangle$, i.e., $\alpha = 0$. It shows that $\gamma_{\mathrm{eff}}^{(\mathrm{c})} \geqslant \gamma_{\mathrm{eff}}^{(\mathrm{n})}$ for all directions of the control Hamiltonian, i.e., any coherent control can only induce decay in the survival probability or keep it unchanged at most, as the system is not affected by the amplitude damping noise and the survival probability cannot benefit from the control Hamiltonian in any direction in this case. Figures 8(a2) and 8(b2) depict the case for the state $|\psi_{\mathrm{b}}\rangle$, i.e., $\alpha = \pi$, and show that $\gamma_{\mathrm{eff}}^{(\mathrm{c})} \leqslant \gamma_{\mathrm{eff}}^{(\mathrm{n})}$ for all directions of the control Hamiltonian, i.e., any coherent control can help slow the decay of survival probability or keep it unchanged at least, as $|1\rangle$ is the state most adversely affected by the amplitude damping noise, and thus the Hamiltonian control in an arbitrary direction can mitigate this situation. Figures 8(a3) and 8(b3) consider the intermediate case with the initial state $|\psi_{\mathrm{c}}\rangle$, i.e., $\alpha = \pi/2$, $\beta = 0$, demonstrating that the possibilities for coherent quantum controls to reduce or increase the decay rate of the survival probability exist simultaneously, as both states that are less or more disturbed by the amplitude damping noise exist on the Bloch sphere in this case.

As the improvement in the decay rate of the survival probability differs among different directions of the control Hamiltonian, it is desirable to find the lowest decay rate by optimizing the control Hamiltonian over all possible directions.

Substituting Eq. (92) into Eq. (84), one can work out the optimal control for the amplitude damping noise, which reveals that for an initial state with a Bloch vector $\boldsymbol{r_0}$ (65) the effective decay rate reaches the minimum when

$$\theta_{\mathrm{c}} = \frac{\alpha}{2}, \quad \phi_{\mathrm{c}} = \beta. \qquad (94)$$

The evolution trajectory of the Bloch vector of the system with the control Hamiltonian in the optimal direction (94) is plotted in Fig. 9.
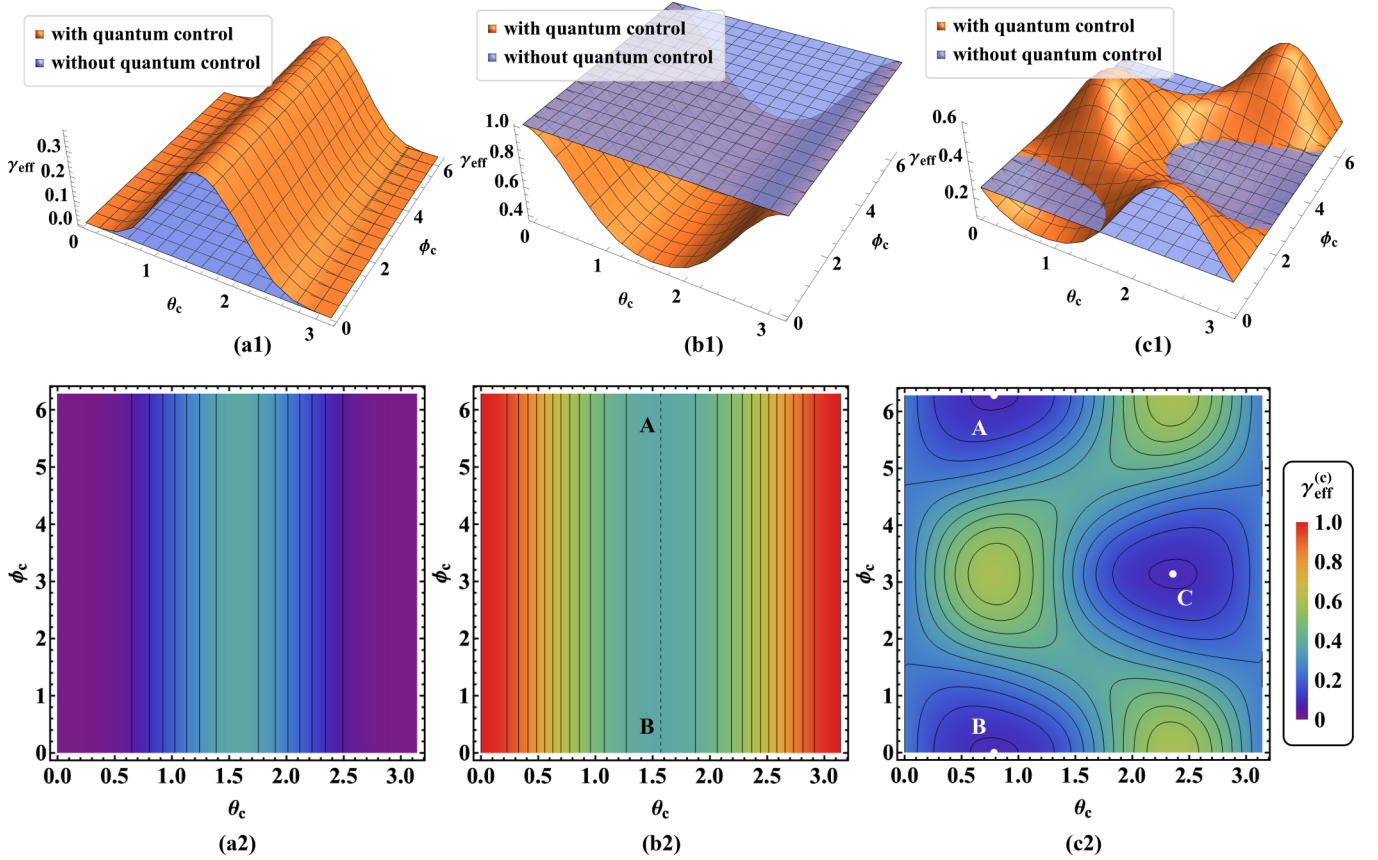
FIG. 8. Illustration of effective decay rates γ_{eff} for different initial states (a) $\alpha_a = 0$, (b) $\alpha_b = \pi$, and (c) $\alpha_c = \pi/2$ in the presence of amplitude damping noise, with the Hamiltonian controls of all possible directions vs without a Hamiltonian control. The decay rates $\gamma_{\text{eff}}^{(n)}$ without the controls are plotted by the blue surface, and the decay rates $\gamma_{\text{eff}}^{(c)}$ with the coherent control are plotted by the orange surface. When the initial state is $\alpha = 0$, the optimal quantum control direction is parallel to the initial state direction $\theta_c = 0$ or π, which is trivial control. When the initial state is $\alpha = \pi$, the direction of the most optimal control can be identified as $\{\theta_c = \pi/2\}$, and the corresponding effective decay rates are represented by the dashed line AB in subfigure (b2). When the initial state is $\alpha = \pi/2$, the optimal controls can be found as $\{\theta_c = \pi/4, \phi_c = 0; \theta_c = 3\pi/4, \phi_c = \pi\}$, and the effective decay rates are represented by the three annotated points A, B, and C in subfigure (c2). Parameters: $\beta = 0$, $\omega = \pi$, and $\mu = 1$.

Similar to the case of dephasing noise, the mechanism of the Hamiltonian control against the amplitude damping noise can be understood from the evolution paths of the quantum system with and without the optimal control, which is illustrated in Fig. 9. The evolution of the system without control is plotted by the black path of Fig. 9, which shows that the quantum system would directly approach the ground state $|0\rangle$ under the influence of amplitude damping noise in this case. However, the rotation under the combined influence of coherent control and amplitude damping noise, shown by the blue path of Fig. 9, suggests that the effect of the coherent control drags the state towards $|0\rangle$, i.e., the north pole of the Bloch sphere, which is the state least influenced by the amplitude damping noise, and then turns it back to the vicinity of the initial state. The result of such a Hamiltonian-controlled evolution ensures the distance between the initial state (point A) and the final state with the control (point C) shorter than that between the initial state and the final state without the control (point B) and thus achieves the purpose of delaying the decay of the quantum system.

With the optimal coherent control scheme in Eq. (94), the effective decay rate of survival probability induced by the amplitude damping noise for any arbitrary initial state can reach its minimum, which turns out to be

$$\gamma_{\text{eff}}^{(\text{opt})} = \frac{3}{8}\mu \sin^4 \frac{\alpha}{2}, \qquad (95)$$

implying that the ratio κ (61) optimized by the coherent control scheme is the same for all initial pure states, which is $\kappa = \gamma_{\text{eff}}^{(\text{opt})}/\gamma_{\text{eff}}^{(n)} = 3/8$. This demonstrates the effectiveness and stability of this optimized coherent quantum control approach. The optimal effective decay rate with the optimal coherent control $\gamma_{\text{eff}}^{(\text{opt})}$ and that without any control $\gamma_{\text{eff}}^{(n)}$ are both independent of the azimuthal angle β of the initial state due to the rotational symmetry of amplitude damping noise. Their relations with the polar angle α of the initial state as well as the best ratio κ is depicted for different initial states in Fig. 10.

If the above optimization approach of the coherent quantum control is applied to each initial state, one can obtain the decay of the ensemble average fidelity F (62) with respect to μt without any quantum control and with the optimal coherent control by substituting Eqs. (91) and (95) into Eq. (87). The
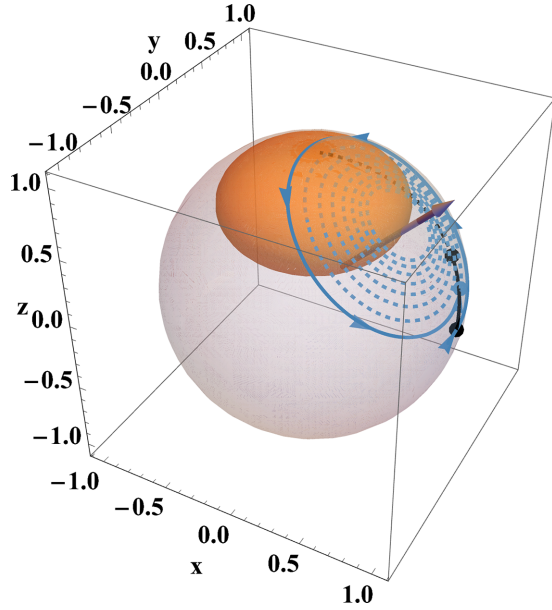
FIG. 9. Evolution paths of a two-level quantum system initially prepared on a pure state with and without the protection of the optimal coherent control between two consecutive projective measurements. The gray, translucent unit sphere represents the set of all density matrices of a two-level system. The deformed, translucent, orange ellipsoid is set of all final density matrices transformed by the amplitude damping noise on the system, and the arrow indicates the direction of optimal coherent control. Point A represents the initial state of the system, and points B and C represent the respective final states after the evolution between two consecutive measurements without and with the optimal coherent quantum control. The black line depicts the evolution path without the control, and the blue line represents the evolution path engineered by the optimal control. The solid arc of the blue line denotes the actual evolution path between two consecutive projective measurements, while the dashed arc of the blue line denotes the future evolution path if the evolution is not interrupted by the repetitive projective measurements. Parameters: $H_0 = \sigma_z, \mu = 1, \omega = \pi, \tau = 0.25$.

ensemble average fidelity is plotted in Fig. 11. It is evident from this figure that the ensemble average fidelity F with the optimal coherent control is always greater than than that without any quantum control, indicating, a decrease in the decay rate of the survival probability by the optimal coherent control. This observation manifests the validity of employing this coherent control scheme to protect the survival probability against the amplitude noise.

Finally, we would like to remark that with the development of quantum technologies in recent years, two-level quantum systems as well as the quantum operations on them have been realized in a variety of physical systems with high precisions, e.g., quantum dots [80], ion traps [81], superconducting quantum circuits [82], etc. We refer the readers to Ref. [83] for a comprehensive review of physical systems that can realize two-level systems and the relevant quantum operations. The coherent controls proposed in the current scheme are essentially unitary rotations of two-level systems on the Bloch sphere, so they can also be implemented on those physical systems.
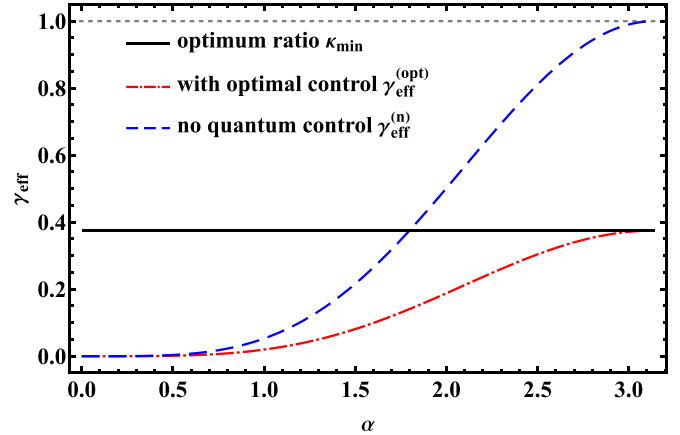

FIG. 10. Illustration of effective decay rates of the survival probability with or without the coherent control in the presence of amplitude damping noise for different initial states. The decay rate $\gamma_{\text{eff}}^{(n)}$ without the coherent control is plotted by the blue dashed line, and the minimum decay rate $\gamma_{\text{eff}}^{(opt)}$ with the optimized coherent control is plotted by the red dot-dashed line. The ratio $\kappa = \gamma_{\text{eff}}^{(opt)}/\gamma_{\text{eff}}^{(n)}$ is also plotted by the black solid line, showing the stability of the optimization performance of this coherent control scheme over different initial states of the system. Parameters: $\omega = \pi$ and $\mu = 1$.

V. CONCLUSION

In this work, we consider the quantum Zeno effect in the presence of noise and study the survival probability that a general quantum system stays in its initial state by repetitive projective measurements in this situation. Starting from the master equation with general dissipative terms, we discuss the physical mechanism underlying the vanishing of the quantum Zeno effect and the decay of the survival probability. In order to suppress the influence of the noise, a coherent control scheme with a strong Hamiltonian is introduced to the quantum system. As the noise induces a nonzero first-order term in the expansion of the survival probability of the initial state which leads the decay of the survival probability, a detailed analysis shows that coherent quantum control with
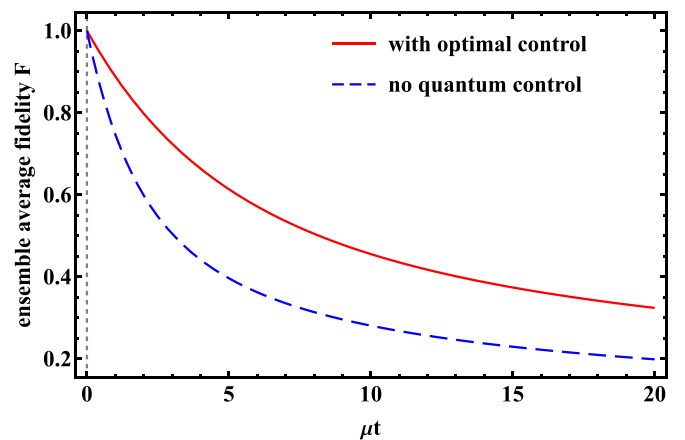

FIG. 11. Ensemble average fidelity F with respect to μt in the presence of amplitude damping noise with or without the optimal coherent quantum control scheme, respectively.

a Hamiltonian as strong as the frequency of the projective measurements can reduce the decay rate of the survival probability. The effective decay rate of the survival probability with the coherent quantum control is obtained, and the conditions on the control Hamiltonian to protect the quantum Zeno effect are established.

A two-level system is then investigated as an example to illustrate the general results. The decay rate of the survival probability is derived with and without the coherent control scheme respectively, and the results indicate that the coherent quantum control scheme performs well in lowering the decay rate in the presence of dephasing and amplitude damping noise. As different control Hamiltonians lead to different suppression effects on the decay of survival probability, the control Hamiltonian is further optimized to minimize the decay rate. An optimization equation for the control Hamiltonian is formally obtained by a variational method and solved analytically for the two types of noise respectively. The mechanism of how the optimal control Hamiltonian protects the system against the noise and mitigates the decay of survival probability is numerically illustrated by visualizing the noisy evolution paths of the quantum system in the Bloch sphere. The results show that the effect of the optimal Hamiltonian control is to rotate the system towards the direction that is least influenced by the noise and then turns it back to the vicinity of the initial state, so that the final state with the optimal control can be closer to the initial state than without the control, and thus the survival probability of the system to stay in the initial state can be increased.

We hope this work can contribute a novel quantum control strategy to mitigate the influence of Markovian noise on the quantum Zeno effect and stimulate future research in this direction.

APPENDIX A: DERIVATION OF REPRESENTATION TRANSFORMATION OF SUPEROPERATORS IN LIOUVILLE SPACE

In this Appendix, we briefly demonstrate how the transformations of superoperators $\mathcal{L}_{H_0}$ and $\mathcal{L}_\mu$ are derived in Eq. (51).

According to the definition of $\mathcal{L}_{H_0}$, $\mathcal{L}_{H_0} = -i[H_0, \cdot]$, and the definition of $e^{\omega \mathcal{L}_{H_c} \eta}$, $e^{\omega \mathcal{L}_{H_c} \eta}[\cdot] = e^{-iH_c\eta}(\cdot)e^{iH_c\eta}$, the transformation of the commutator $\mathcal{L}_{H_0}$ into a representation rotated by $e^{-\omega \mathcal{L}_{H_c} \eta}$ is

$$
\begin{aligned}
&e^{-\omega \mathcal{L}_{H_c}\eta}\mathcal{L}_{H_0}e^{\omega \mathcal{L}_{H_c}\eta}[\cdot]\\
&= -i e^{i\omega H_c\eta}[H_0 e^{-i\omega H_c\eta}(\cdot)e^{i\omega H_c\eta} - e^{-i\omega H_c\eta}(\cdot)e^{i\omega H_c\eta}H_0]e^{-i\omega H_c\eta}\\
&= -i[e^{i\omega H_c\eta}H_0 e^{-i\omega H_c\eta}, \cdot]\\
&= -i[\widetilde{H}_0(\eta), \cdot] = \widetilde{\mathcal{L}}_{H_0}^{(\eta)},
\end{aligned}
\tag{A1}
$$

where $\widetilde{H}_0(\eta) = e^{i\omega H_c\eta}H_0 e^{-i\omega H_c\eta}$ is the transformed free Hamiltonian in the rotated representation dependent on the parameter η, and the transformation of the dissipative superoperator $\mathcal{L}_\mu$ is

$$
\begin{aligned}
&e^{-\omega \mathcal{L}_{H_c}\eta}\mathcal{L}_\mu e^{\omega \mathcal{L}_{H_c}\eta}[\cdot]\\
&= \sum_k \mu_k e^{-\omega \mathcal{L}_{H_c}\eta}\mathcal{D}[V_k]e^{\omega \mathcal{L}_{H_c}\eta}(\cdot)\\
&= \sum_k \mu_k e^{i\omega H_c\eta}\bigg\{V_k[e^{-i\omega H_c\eta}(\cdot)e^{i\omega H_c\eta}]V_k^\dagger\\
&\quad -\frac{1}{2}V_k^\dagger V_k[e^{-i\omega H_c\eta}(\cdot)e^{i\omega H_c\eta}]\\
&\quad -\frac{1}{2}[e^{-i\omega H_c\eta}(\cdot)e^{i\omega H_c\eta}]V_k^\dagger V_k\bigg\}e^{-i\omega H_c\eta}\\
&= \sum_k \mu_k\bigg[\widetilde{V}_k(\eta)(\cdot)\widetilde{V}_k^\dagger(\eta) - \frac{1}{2}\{\widetilde{V}_k^\dagger(\eta)\widetilde{V}_k(\eta), \cdot\}\bigg]\\
&= \sum_k \mu_k \mathcal{D}[\widetilde{V}_k(\eta)],
\end{aligned}
\tag{A2}
$$

where $\widetilde{V}_k(\eta) = e^{i\omega H_c\eta}V_k e^{-i\omega H_c\eta}$ is the transformed noise operator V_k in the framework rotated by $e^{-i\omega H_c\eta}$ dependent on the parameter η.

It can be observed that the transformations of the superoperators $\mathcal{L}_{H_0}$ and $\mathcal{L}_\mu$ are essentially the transformations of the free Hamiltonian H_0 and the noise operators V_k under the control Hamiltonian H_c, respectively, while the forms of $\mathcal{L}_{H_0}$ and $\mathcal{L}_\mu$, regardless of H_0 and V_k, remain unchanged.

APPENDIX B: DERIVATION OF OPTIMIZATION EQUATION FOR CONTROL HAMILTONIAN

In this Appendix, we derive the equation that determine the optimal control Hamiltonians to minimize the effective decay rates of survival probability $\gamma_{\text{eff}}^{(c)}$ for a two-level quantum system.

We start from the general result for $\gamma_{\text{eff}}^{(c)}$,

$$
\begin{aligned}
\gamma_{\text{eff}}^{(c)} = &-\tfrac{3}{2}(\boldsymbol{n_c} \cdot \boldsymbol{r_0})^2 \boldsymbol{n_c}\Gamma \boldsymbol{n_c} + \tfrac{1}{2}\boldsymbol{n_c} \cdot \boldsymbol{r_0}(\boldsymbol{n_c}\Gamma \boldsymbol{r_0} + \boldsymbol{r_0}\Gamma \boldsymbol{n_c}) - \tfrac{1}{2}\boldsymbol{r_0}\Gamma \boldsymbol{r_0}\\
&-\tfrac{1}{2}(\boldsymbol{n_c} \times \boldsymbol{r_0})\Gamma(\boldsymbol{n_c} \times \boldsymbol{r_0}) + \text{Tr}\Gamma + (\boldsymbol{n_c} \cdot \boldsymbol{r_0})(\mathbf{g} \cdot \mathbf{n_c}),
\end{aligned}
\tag{B1}
$$

which is provided by Eq. (73) in Sec. IV B.

Denote the Bloch vector of the initial state as $\boldsymbol{r_0}$ and the normalized directional vector of the control Hamiltonian as $\boldsymbol{n_c}$, i.e., $H_c = \boldsymbol{n_c} \cdot \boldsymbol{\sigma}$. The cross product between the vectors $\boldsymbol{n_c}$ and $\boldsymbol{r_0}$ can be represented as a linear transformation of $\boldsymbol{n_c}$, given by

$$
\boldsymbol{n_c} \times \boldsymbol{r_0} = R\boldsymbol{n_c}.
\tag{B2}
$$

If $\boldsymbol{r_0}$ is denoted as

$$
\boldsymbol{r_0} = (x_0, y_0, z_0),
\tag{B3}
$$

the transformation matrix R is antisymmetric and defined as

$$
R = \begin{bmatrix} 0 & z_0 & -y_0 \\ -z_0 & 0 & x_0 \\ y_0 & -x_0 & 0 \end{bmatrix}.
\tag{B4}
$$

In this case, the effective decay rate of survival probability $\gamma_{\text{eff}}^{(c)}$ can be rewritten as

$$
\begin{aligned}
\gamma_{\text{eff}}^{(c)} &= -\frac{3}{2}(\boldsymbol{r_0^{\mathrm{T}} n_c})(\boldsymbol{n_c^{\mathrm{T}}} \Gamma \boldsymbol{n_c})(\boldsymbol{n_c^{\mathrm{T}} r_0}) + \frac{1}{2}(\boldsymbol{r_0^{\mathrm{T}} n_c})(\boldsymbol{n_c^{\mathrm{T}}} \Gamma \boldsymbol{r_0}) \\
&\quad + \frac{1}{2}(\boldsymbol{r_0^{\mathrm{T}}} \Gamma \boldsymbol{n_c})(\boldsymbol{n_c^{\mathrm{T}} r_0}) - \frac{1}{2}\boldsymbol{r_0^{\mathrm{T}}} \Gamma \boldsymbol{r_0} \\
&\quad - \frac{1}{2}(R\boldsymbol{n_c})^{\mathrm{T}} \Gamma(R\boldsymbol{n_c}) + \mathrm{Tr}\,\Gamma + (\boldsymbol{v^{\mathrm{T}} n_c})(\boldsymbol{n_c^{\mathrm{T}} r_0}) \\
&= \mathrm{Tr}\bigg(-\frac{3}{2}P_n \Gamma P_n P_r + \frac{1}{2}P_n \Gamma P_r + \frac{1}{2}\Gamma P_n P_r \\
&\quad - \frac{1}{2}\Gamma P_r - \frac{1}{2}R^{\mathrm{T}} \Gamma R P_n + \Gamma + P_n \boldsymbol{r_0} \boldsymbol{v^{\mathrm{T}}}\bigg), \quad \text{(B5)}
\end{aligned}
$$

where P_n and P_r are defined as $P_n = \boldsymbol{n_c n_c^{\mathrm{T}}}$ and $P_r = \boldsymbol{r_0 r_0^{\mathrm{T}}}$, respectively, and the superscript "T" denotes the transposition of a column vector.

Considering the normalization of the vector $\boldsymbol{n_c}$, i.e., $\|\boldsymbol{n_c}\| = 1$, P_n is actually a projection operator, satisfying $P_n^2 = P_n$, so the Lagrangian function should include this property of P_n as a constraint condition,

$$
L(P_n, \Lambda) = \gamma_{\text{eff}}^{(c)} + \mathrm{Tr}\big[\big(P_n^2 - P_n\big)\Lambda\big], \quad \text{(B6)}
$$

where Λ is an arbitrary matrix, representing the Lagrange multiplier.

To obtain the optimal control Hamiltonian H_c that minimizes the effective decay rate $\gamma_{\text{eff}}^{(c)}$, we perform variational calculus on the Lagrangian function (B6), yielding

$$
\begin{aligned}
\delta L &= \mathrm{Tr}\bigg[\delta P_n\bigg(-\frac{3}{2}\Gamma P_n P_r - \frac{3}{2}P_r P_n \Gamma + \frac{1}{2}\Gamma P_r + \frac{1}{2}P_r \Gamma \\
&\quad - \frac{1}{2}R^{\mathrm{T}} \Gamma R + \boldsymbol{r_0} \boldsymbol{v^{\mathrm{T}}} + P_n \Lambda + \Lambda P_n - \Lambda\bigg)\bigg] \\
&\quad + \mathrm{Tr}\big[\delta \Lambda \big(P_n^2 - P_n\big)\big]. \quad \text{(B7)}
\end{aligned}
$$

According to the principle of the variational approach, the variation δL in Eq. (B7) should be zero for any δP_n and $\delta \Lambda$, leading to the following conditions for minimizing the effective decay rate $\gamma_{\text{eff}}^{(c)}$:

$$
\begin{aligned}
&-\frac{3}{2}\Gamma P_n P_r - \frac{3}{2}P_r P_n \Gamma + \frac{1}{2}\Gamma P_r + \frac{1}{2}P_r \Gamma \\
&-\frac{1}{2}R^{\mathrm{T}} \Gamma R + \boldsymbol{r_0} \boldsymbol{v^{\mathrm{T}}} + P_n \Lambda + \Lambda P_n - \Lambda = \boldsymbol{0}, \quad \text{(B8)}
\end{aligned}
$$

$$
P_n^2 - P_n = \boldsymbol{0}, \quad \text{(B9)}
$$

where the bold symbol $\boldsymbol{0}$ denotes the zero matrix.

APPENDIX C: DERIVATION OF EFFECTIVE DECAY RATE OF SURVIVAL PROBABILITY FOR TWO-LEVEL SYSTEM

This Appendix focuses primarily on the coherent control scheme for two-level system, specifically the derivations discussed in Sec. IV. We start from the general results of effective decay rates $\gamma_{\text{eff}}^{(n)}$ (29) without quantum control and $\gamma_{\text{eff}}^{(c)}$ (60) with coherent quantum controls in Sec. III, and apply them to a two-level system in the presence of Markovian noise with and without the coherent control scheme respectively.

The dissipative superoperator $\mathcal{L}_\mu$ induced by Markovian noise for a two-level system can be generally expressed as

$$
\mathcal{L}_\mu[\cdot] = \sum_{ij} \mu_{ij}\bigg(\sigma_i(\cdot)\sigma_j - \frac{1}{2}\{\sigma_j \sigma_i, \cdot\}\bigg), \quad \text{(C1)}
$$

which is given in Eq. (66). By substituting this equation into $\gamma_{\text{eff}}^{(n)}$ (29), one can derive the effective decay rate for a noisy two-level quantum system without quantum control as

$$
\begin{aligned}
\gamma_{\text{eff}}^{(n)} &= -\langle \psi_0 | \mathcal{L}_\mu[\rho_0] | \psi_0 \rangle \\
&= -\sum_{i,j=1,2} \mu_{ij} \mathrm{Tr}\bigg(\rho_0 \sigma_i \rho_0 \sigma_j - \frac{1}{2}\rho_0\{\sigma_j \sigma_i, \rho_0\}\bigg) \\
&= -\sum_{i,j=1,2} \mu_{ij}[\mathrm{Tr}(\sigma_i \rho_0)\mathrm{Tr}(\sigma_j \rho_0) - \mathrm{Tr}(\sigma_j \sigma_i \rho_0)], \\
&= -\boldsymbol{r_0^{\mathrm{T}}} \Gamma \boldsymbol{r_0} + \mathrm{Tr}\,\Gamma - i\sum_{ijk} \mu_{ij} \varepsilon_{ijk}(r_0)_k \\
&= -\boldsymbol{r_0^{\mathrm{T}}} \Gamma \boldsymbol{r_0} + \mathrm{Tr}\,\Gamma + \boldsymbol{v} \cdot \boldsymbol{r_0}, \quad \text{(C2)}
\end{aligned}
$$

where the third line of the derivation results from the assumption that ρ_0 is the density matrix of a pure state, $\boldsymbol{v}$ is a vector related to the imaginary parts of the off-diagonal elements of the noise coefficient matrix Γ, defined as

$$
\boldsymbol{v} = 2(\mathrm{Im}\mu_{23}, \mathrm{Im}\mu_{31}, \mathrm{Im}\mu_{12}). \quad \text{(C3)}
$$

In the coherent control scheme, we assume that the control Hamiltonian can be written as

$$
H_c = \boldsymbol{n_c} \cdot \boldsymbol{\sigma}, \quad \text{(C4)}
$$

where $\boldsymbol{n_c}$ describes the direction of the control Hamiltonian,

$$
\boldsymbol{n_c} = (\sin\theta_c \cos\phi_c, \sin\theta_c \sin\phi_c, \cos\theta_c). \quad \text{(C5)}
$$

The eigenvalues and the associated eigenstates of the control Hamiltonian H_c can be straightforwardly obtained as

$$
\begin{aligned}
E_1^{(c)} &= 1, \quad \big|\psi_1^{(c)}\big\rangle = e^{-i\phi_c}\cos\frac{\theta_c}{2}|0\rangle + \sin\frac{\theta_c}{2}|1\rangle \\
E_2^{(c)} &= -1, \quad \big|\psi_2^{(c)}\big\rangle = -e^{-i\phi_c}\sin\frac{\theta_c}{2}|0\rangle + \cos\frac{\theta_c}{2}|1\rangle
\end{aligned}, \quad \text{(C6)}
$$

where $E_1^{(c)}$, $E_2^{(c)}$ are the eigenvalues and $|\psi_1^{(c)}\rangle$, $|\psi_2^{(c)}\rangle$ are the eigenstates.

Correspondingly, an arbitrary initial state $|\psi_0\rangle$ in the basis of the Hamiltonian's eigenstates can be expressed as

$$
|\psi_0\rangle = a_1\big|\psi_1^{(c)}\big\rangle + a_2\big|\psi_2^{(c)}\big\rangle, \quad \text{(C7)}
$$

where the coefficients a_1, a_2 satisfy the normalization condition $|a_1|^2 + |a_2|^2 = 1$.

Now, let us derive the effective decay rate $\gamma_{\text{eff}}^{(c)}$ for a two-level system within scheme with the coherent quantum control. The first consideration pertains to the necessary conditions for the validity of the coherent control scheme in a two-level system. Substituting the eigenvalues from Eq. (C6) into the zeroth-order term of survival probability $p_c(\tau)$ in Eq. (41), one can have

$$
\begin{aligned}
p_c|_{\tau=0} &= |\langle \psi_0 | e^{i\omega H_c} | \psi_0 \rangle|^2 \\
&= |a_1|^4 + |a_2|^4 + 2|a_1|^2|a_2|^2 \cos 2\omega, \quad \text{(C8)}
\end{aligned}
$$

indicating that when $\omega = n\pi$ for $n = \pm 1, \pm 2, \pm 3, \ldots$, $p_c|_{\tau=0} = 1$ by the normalization condition of a_1, a_2.

With the specific form of $\mathcal{L}_\mu$ for a two-level system given in Eq. (C1) and the representation transformation of superoperator $\mathcal{L}_\mu$, $\widetilde{\mathcal{L}}_\mu^{(\eta)} = e^{-\omega \mathcal{L}_{H_c} \eta} \mathcal{L}_\mu e^{\omega \mathcal{L}_{H_c} \eta}$, in Eq. (A2), the first-order term of Eq. (41) can be written as

$$p_c^{(1)}|_{\tau=0} = \int_0^1 \langle \psi_0 | \widetilde{\mathcal{L}}_\mu^{(\eta)}[\rho_0] | \psi_0 \rangle \, d\eta$$

$$= \sum_{i,j=1}^3 \mu_{ij} \int_0^1 \mathrm{Tr}\big[\rho_0 \widetilde{\sigma}_i^{(\eta)} \rho_0 \widetilde{\sigma}_j^{(\eta)} - \rho_0 \widetilde{\sigma}_j^{(\eta)} \widetilde{\sigma}_i^{(\eta)}\big] d\eta,$$

$$\text{(C9)}$$

where $\widetilde{\sigma}_i^{(\eta)} \equiv e^{i\omega H_c \eta} \sigma_i e^{-i\omega H_c \eta}$ denotes the Pauli operator σ_i in the transformed framework. As H_c is a normalized Pauli matrix defined in (C4), satisfying $H_c^2 = I$, one can have

$$e^{\pm i\omega H_c \eta} = \cos(\omega\eta)\mathbb{I} \pm i \sin(\omega\eta) H_c. \qquad \text{(C10)}$$

Considering the necessary condition $\omega = n\pi$, $n = \pm 1$, $\pm 2, \pm 3, \ldots$, substituting the above equation, $H_c = \boldsymbol{n_c} \cdot \boldsymbol{\sigma}$, and $\rho_0 = (\mathbb{I} + \boldsymbol{r_0} \cdot \boldsymbol{\sigma})/2$ into Eq. (C9) and using the identity

$$(\boldsymbol{a} \cdot \boldsymbol{\sigma})(\boldsymbol{b} \cdot \boldsymbol{\sigma}) = (\boldsymbol{a} \cdot \boldsymbol{b})\,\mathbb{I} + i(\boldsymbol{a} \times \boldsymbol{b}) \cdot \boldsymbol{\sigma}, \qquad \text{(C11)}$$

for two arbitrary vectors $\boldsymbol{a}$ and $\boldsymbol{b}$, one can obtain

$$p_c^{(1)}\big|_{\tau=0} = \sum_{i,j=1}^3 \mu_{ij} \int_0^1 \mathrm{Tr}(\rho_0 e^{i\omega H_c \eta} \sigma_i e^{-i\omega H_c \eta} \rho_0 e^{i\omega H_c \eta} \sigma_j e^{-i\omega H_c \eta} - \rho_0 e^{i\omega H_c \eta} \sigma_j \sigma_i e^{-i\omega H_c \eta}) d\eta \qquad \text{(C12)}$$

$$= \sum_{i,j=1}^3 \mu_{ij} \bigg\{ \int_0^1 \mathrm{Tr}\big(\rho_0 [\cos(\omega\eta)\,\mathbb{I} + i\sin(\omega\eta)\,\boldsymbol{n_c} \cdot \boldsymbol{\sigma}] \sigma_i [\cos(\omega\eta)\,\mathbb{I} - i\sin(\omega\eta)\,\boldsymbol{n_c} \cdot \boldsymbol{\sigma}] \rho_0$$

$$\times [\cos(\omega\eta)\,\mathbb{I} + i\sin(\omega\eta)\,\boldsymbol{n_c} \cdot \boldsymbol{\sigma}] \sigma_j [\cos(\omega\eta)\,\mathbb{I} + i\sin(\omega\eta)\,\boldsymbol{n_c} \cdot \boldsymbol{\sigma}] d\eta\big)$$

$$- \int_0^1 \mathrm{Tr}\big(\rho_0 [\cos(\omega\eta)\,\mathbb{I} + i\sin(\omega\eta)\,\boldsymbol{n_c} \cdot \boldsymbol{\sigma}] \sigma_j \sigma_i [\cos(\omega\eta)\,\mathbb{I} - i\sin(\omega\eta)\,\boldsymbol{n_c} \cdot \boldsymbol{\sigma}] d\eta\big) \bigg\} \qquad \text{(C13)}$$

$$= \sum_{i,j=1}^3 \mu_{ij} \bigg\{ \frac{3}{2}(\boldsymbol{n_c} \cdot \boldsymbol{r_0})^2 (\boldsymbol{n_c})_i (\boldsymbol{n_c})_j - \frac{1}{2} \boldsymbol{n_c} \cdot \boldsymbol{r_0}\big[(\boldsymbol{n_c})_i (\boldsymbol{r_0})_j + (\boldsymbol{r_0})_i (\boldsymbol{n_c})_j\big] + \frac{1}{2}(\boldsymbol{r_0})_i (\boldsymbol{r_0})_j$$

$$+ \frac{1}{2}(\boldsymbol{n_c} \times \boldsymbol{r_0})_i (\boldsymbol{n_c} \times \boldsymbol{r_0})_j - \delta_{ij} + i(\boldsymbol{n_c} \cdot \boldsymbol{r_0}) \sum_k \varepsilon_{ijk} (\boldsymbol{n_c})_k \bigg\}, \qquad \text{(C14)}$$

where $(\boldsymbol{n_c})_k$, $(\boldsymbol{r_0})_k$, and $(\boldsymbol{n_c} \times \boldsymbol{r_0})_k$ denote the kth elements of vectors $\boldsymbol{n_c}$, $\boldsymbol{r_0}$, and $\boldsymbol{n_c} \times \boldsymbol{r_0}$, respectively.

Substituting the real vector $\boldsymbol{v}$ defined in Eq. (C3) into the above equation, one can finally arrive at

$$p_c^{(1)}\big|_{\tau=0} = \frac{3}{2}(\boldsymbol{n_c} \cdot \boldsymbol{r_0})^2 \boldsymbol{n_c^T} \Gamma \boldsymbol{n_c} - \frac{1}{2}(\boldsymbol{n_c} \cdot \boldsymbol{r_0})(\boldsymbol{n_c^T} \Gamma \boldsymbol{r_0} + \boldsymbol{r_0^T} \Gamma \boldsymbol{n_c}) + \frac{1}{2}\boldsymbol{r_0^T} \Gamma \boldsymbol{r_0}$$

$$+ \frac{1}{2}(\boldsymbol{n_c} \times \boldsymbol{r_0})^T \Gamma (\boldsymbol{n_c} \times \boldsymbol{r_0}) - \mathrm{Tr}\Gamma - (\boldsymbol{n_c} \cdot \boldsymbol{r_0})(\boldsymbol{v} \cdot \boldsymbol{n_c}), \qquad \text{(C15)}$$

which is Eq. (73).

[1] Aristotle, *The Complete Works of Aristotle Physics Book VI 239b5*, edited by J. Barnes, Bollingen Series Edition (Princeton University Press, Princeton, NJ, 1984).

[2] J. von Neumann, *Mathematische Grundlagen der Quantenmechanik* (Springer, Berlin, 1932).

[3] A. Beskow and J. Nilsson, Ark. Fys. **34**, 561 (1967).

[4] W. M. Itano, D. J. Heinzen, J. J. Bollinger, and D. J. Wineland, Phys. Rev. A **41**, 2295 (1990).

[5] P. Kwiat, H. Weinfurter, T. Herzog, A. Zeilinger, and M. A. Kasevich, Phys. Rev. Lett. **74**, 4763 (1995).

[6] B. Nagels, L. J. F. Hermans, and P. L. Chapovsky, Phys. Rev. Lett. **79**, 3097 (1997).

[7] E. W. Streed, J. Mun, M. Boyd, G. K. Campbell, P. Medley, W. Ketterle, and D. E. Pritchard, Phys. Rev. Lett. **97**, 260402 (2006).

[8] J. Bernu, S. Deléglise, C. Sayrin, S. Kuhr, I. Dotsenko, M. Brune, J. M. Raimond, and S. Haroche, Phys. Rev. Lett. **101**, 180402 (2008).

[9] A. Signoles, A. Facon, D. Grosso, I. Dotsenko, S. Haroche, J.-M. Raimond, M. Brune, and S. Gleyzes, Nat. Phys. **10**, 715 (2014).

[10] F. Schäfer, I. Herrera, S. Cherukattil, C. Lovecchio, F. S. Cataliotti, F. Caruso, and A. Smerzi, Nat. Commun. **5**, 3194 (2014).

[11] D. H. Slichter, C. Müller, R. Vijay, S. J. Weber, A. Blais, and I. Siddiqi, New J. Phys. **18**, 053031 (2016).

[12] P. Exner and T. Ichinose, Ann. Henri Poincaré **6**, 195 (2005).

[13] P. Exner, T. Ichinose, H. Neidhardt, and V. A. Zagrebnov, Integral Equ. Operator Theory **57**, 67 (2007).

[14] D. Burgarth, P. Facchi, G. Gramegna, and S. Pascazio, J. Phys. A: Math. Theor. **52**, 435301 (2019).

[15] P. Exner and T. Ichinose, Ann. Henri Poincaré **22**, 1669 (2021).

[16] B. Misra and E. C. G. Sudarshan, J. Math. Phys. **18**, 756 (1977).

[17] K. Koshino and A. Shimizu, Phys. Rep. **412**, 191 (2005).

[18] P. Facchi and S. Pascazio, J. Phys. A: Math. Theor. **41**, 493001 (2008).

[19] B. Kaulakys and V. Gontis, Phys. Rev. A **56**, 1131 (1997).

[20] A. G. Kofman and G. Kurizki, Nature (London) **405**, 546 (2000).

[21] P. Facchi, H. Nakazato, and S. Pascazio, Phys. Rev. Lett. **86**, 2699 (2001).

[22] P. Facchi and S. Pascazio, Phys. Rev. Lett. **89**, 080401 (2002).

[23] J. M. Raimond, C. Sayrin, S. Gleyzes, I. Dotsenko, M. Brune, S. Haroche, P. Facchi, and S. Pascazio, Phys. Rev. Lett. **105**, 213601 (2010).

[24] G. A. Paz-Silva, A. T. Rezakhani, J. M. Dominy, and D. A. Lidar, Phys. Rev. Lett. **108**, 080501 (2012).

[25] D. Burgarth, P. Facchi, H. Nakazato, S. Pascazio, and K. Yuasa, Quantum **4**, 289 (2020).

[26] L. Viola, Phys. Rev. A **58**, 2733 (1998).

[27] L. Viola, E. Knill, and S. Lloyd, Phys. Rev. Lett. **82**, 2417 (1999).

[28] L.-M. Duan and G.-C. Guo, Phys. Lett. A **261**, 139 (1999).

[29] P. Facchi, D. A. Lidar, and S. Pascazio, Phys. Rev. A **69**, 032314 (2004).

[30] L. S. Schulman, Phys. Rev. A **57**, 1509 (1998).

[31] H. Nakazato and S. Pascazio, J. Supercond. **12**, 843 (1999).

[32] K. Macieszczak, M. Guţă, I. Lesanovsky, and J. P. Garrahan, Phys. Rev. Lett. **116**, 240404 (2016).

[33] K. Snizhko, P. Kumar, and A. Romito, Phys. Rev. Res. **2**, 033512 (2020).

[34] K. Kumari, G. Rajpoot, S. Joshi, and S. R. Jain, Ann. Phys. **450**, 169222 (2023).

[35] R. Ruskov, A. N. Korotkov, and A. Mizel, Phys. Rev. B **73**, 085317 (2006).

[36] S. Gherardini, S. Gupta, F. S. Cataliotti, A. Smerzi, F. Caruso, and S. Ruffo, New J. Phys. **18**, 013048 (2016).

[37] P. Kumar, A. Romito, and K. Snizhko, Phys. Rev. Res. **2**, 043420 (2020).

[38] B. Elattari and S. A. Gurvitz, Phys. Rev. Lett. **84**, 2047 (2000).

[39] S. A. Gurvitz, L. Fedichkin, D. Mozyrsky, and G. P. Berman, Phys. Rev. Lett. **91**, 066801 (2003).

[40] C. Presilla, R. Onofrio, and U. Tambini, Ann. Phys. **248**, 95 (1996).

[41] P. Facchi, S. Tasaki, S. Pascazio, H. Nakazato, A. Tokuse, and D. A. Lidar, Phys. Rev. A **71**, 022302 (2005).

[42] D. Burgarth, P. Facchi, H. Nakazato, S. Pascazio, and K. Yuasa, Quantum **3**, 152 (2019).

[43] A. Hahn, D. Burgarth, and K. Yuasa, New J. Phys. **24**, 063027 (2022).

[44] *Decoherence: Theoretical, Experimental, and Conceptual Problems*, 2000 ed., edited by P. Blanchard, D. Giulini, E. Joos, C. Kiefer, and I.-O. Stamatescu (Springer, Berlin, 2000).

[45] D. Braun, *Dissipative Quantum Chaos and Decoherence*, 2001 ed. (Springer, Berlin, 2013).

[46] S. Gurvitz, Quantum Inf. Proc. **2**, 15 (2003).

[47] C. A. E. Guerra, D. V. Villamizar, and L. G. C. Rego, Phys. Rev. A **86**, 023411 (2012).

[48] L.-M. Duan and G.-C. Guo, Phys. Rev. A **57**, 737 (1998).

[49] A. Shabani and D. A. Lidar, Phys. Rev. A **72**, 042303 (2005).

[50] D. A. Lidar and K. Birgitta Whaley, in *Irreversible Quantum Dynamics*, edited by F. Benatti and R. Floreanini, Lecture Notes in Physics (Springer, Berlin, 2003), pp. 83–120.

[51] A. P. Peirce, M. A. Dahleh, and H. Rabitz, Phys. Rev. A **37**, 4950 (1988).

[52] R. S. Judson and H. Rabitz, Phys. Rev. Lett. **68**, 1500 (1992).

[53] P. W. Shor, Phys. Rev. A **52**, R2493 (1995).

[54] A. M. Steane, Phys. Rev. Lett. **77**, 793 (1996).

[55] L. Vaidman, L. Goldenberg, and S. Wiesner, Phys. Rev. A **54**, R1745 (1996).

[56] L.-M. Duan and G.-C. Guo, Phys. Rev. A **57**, 2399 (1998).

[57] C.-P. Yang, S.-I. Chu, and S. Han, Phys. Rev. A **66**, 034301 (2002).

[58] N. Erez, Y. Aharonov, B. Reznik, and L. Vaidman, Phys. Rev. A **69**, 062315 (2004).

[59] A. Beige, D. Braun, B. Tregenna, and P. L. Knight, Phys. Rev. Lett. **85**, 1762 (2000).

[60] K. Stannigel, P. Hauke, D. Marcos, M. Hafezi, S. Diehl, M. Dalmonte, and P. Zoller, Phys. Rev. Lett. **112**, 120406 (2014).

[61] S. Patsch, S. Maniscalco, and C. P. Koch, Phys. Rev. Res. **2**, 023133 (2020).

[62] S. Virzì, A. Avella, F. Piacentini, M. Gramegna, T. Opatrný, A. G. Kofman, G. Kurizki, S. Gherardini, F. Caruso, I. P. Degiovanni, and M. Genovese, Phys. Rev. Lett. **129**, 030401 (2022).

[63] E. Blumenthal, C. Mor, A. A. Diringer, L. S. Martin, P. Lewalle, D. Burgarth, K. B. Whaley, and S. Hacohen-Gourgy, npj Quantum Inf. **8**, 88 (2022).

[64] D. Herman, R. Shaydulin, Y. Sun, S. Chakrabarti, S. Hu, P. Minssen, A. Rattew, R. Yalovetzky, and M. Pistoia, Commun. Phys. **6**, 219 (2023).

[65] V. Popkov, S. Essink, C. Presilla, and G. Schütz, Phys. Rev. A **98**, 052110 (2018).

[66] V. Popkov and C. Presilla, Phys. Rev. Lett. **126**, 190402 (2021).

[67] G. Lindblad, Commun. Math. Phys. **48**, 119 (1976).

[68] V. Gorini, A. Kossakowski, and E. C. G. Sudarshan, J. Math. Phys. **17**, 821 (1976).

[69] H.-P. Breuer and F. Petruccione, *The Theory of Open Quantum Systems* (Oxford University Press, New York, 2007).

[70] R. Alicki and K. Lendi, *Quantum Dynamical Semigroups and Applications*, Lecture Notes in Physics Vol. 286 (Springer-Verlag, Berlin, Heidelberg, 1987).

[71] D. Chruściński and S. Pascazio, Open Syst. Inf. Dyn. **24**, 1740001 (2017).

[72] Á. Rivas and S. F. Huelga, *Open Quantum Systems: An Introduction* (Springer, Berlin, 2012).

[73] H. Zheng, S. Y. Zhu, and M. S. Zubairy, Phys. Rev. Lett. **101**, 200404 (2008).

[74] J.-M. Zhang, J. Jing, L.-G. Wang, and S.-Y. Zhu, Phys. Rev. A **98**, 012135 (2018).

[75] J. A. Gyamfi, Eur. J. Phys. **41**, 063002 (2020).

[76] W. Yang and R.-B. Liu, Phys. Rev. Lett. **101**, 180403 (2008).

[77] R. M. Wilcox, J. Math. Phys. **8**, 962 (1967).

[78] M. A. Nielsen and I. L. Chuang, *Quantum Computation and Quantum Information* (Cambridge University Press, New York, 2000).

[79] M. S. Bazaraa, *Nonlinear Programming: Theory and Algorithms*, 3rd ed. (Wiley Publishing, New Jersey, 2013).

[80] G. Burkard, T. D. Ladd, A. Pan, J. M. Nichol, and J. R. Petta, Rev. Mod. Phys. **95**, 025003 (2023).

[81] C. D. Bruzewicz, J. Chiaverini, R. McConnell, and J. M. Sage, Appl. Phys. Rev. **6**, 021314 (2019).

[82] A. Blais, A. L. Grimsmo, S. M. Girvin, and A. Wallraff, Rev. Mod. Phys. **93**, 025005 (2021).

[83] G. Chen, D. A. Church, B.-G. Englert, C. Henkel, B. Rohwedder, M. O. Scully, and M. S. Zubairy, *Quantum Computing Devices: Principles, Designs, and Analysis* (Chapman and Hall/CRC, New York, 2006).